

MIT Open Access Articles

*Response and Resistance to NF- κ B Inhibitors
in Mouse Models of Lung Adenocarcinoma*

The MIT Faculty has made this article openly available. **Please share**
how this access benefits you. Your story matters.

Citation: Richardson, Claire E., Tristan Kooistra, and Dennis H. Kim. "An essential role for XBP-1 in host protection against immune activation in *C. elegans*." *Nature* 463 (2010): 1092-1095.

As Published: <http://dx.doi.org/10.1158/2159-8290.CD-11-0073>

Publisher: American Association for Cancer Research

Persistent URL: <http://hdl.handle.net/1721.1/66545>

Version: Author's final manuscript: final author's manuscript post peer review, without publisher's formatting or copy editing

Terms of use: Creative Commons Attribution-Noncommercial-Share Alike 3.0



Response and resistance to NF-κB inhibitors in mouse models of lung adenocarcinoma

Wen Xue¹, Etienne Meylan^{1,3}, Trudy G. Oliver¹, David M. Feldser¹, Monte M. Winslow¹, Roderick Bronson², Tyler Jacks¹

¹Koch Institute for Integrative Cancer Research, Department of Biology, and Howard Hughes Medical Institute, Massachusetts Institute of Technology, 77 Massachusetts Avenue, Cambridge, Massachusetts 02139, USA.

²Tufts University, and Harvard Medical School, 77 Avenue Louis Pasteur, Boston, Massachusetts 02115, USA.

³Current Address: Swiss Institute for Experimental Cancer Research, Ecole Polytechnique Fédérale de Lausanne, Station 19, CH-1015 Lausanne, Switzerland

Abstract:

Lung adenocarcinoma is a frequently diagnosed cancer type and a leading cause of cancer death worldwide. We recently demonstrated in an autochthonous mouse model of this disease that genetic inhibition of the NF-κB pathway affects both the initiation and maintenance of lung cancer, identifying this pathway as a promising therapeutic target. In this study, we tested the efficacy of small molecule NF-κB inhibitors in mouse models of lung cancer. In murine lung adenocarcinoma cell lines with high NF-κB activity, the proteasome inhibitor Bortezomib efficiently reduced nuclear p65, repressed NF-κB target genes and rapidly induced apoptosis. Bortezomib also induced lung tumor regression *in vivo* and prolonged the survival of tumor bearing *Kras*^{LSL-G12D/wt};*p53*^{flox/flox} mice. In contrast, *Kras*^{G12D/wt} lung tumors, which have low levels

of nuclear NF- κ B, do not respond to Bortezomib, suggesting that nuclear NF- κ B may be a biomarker to predict treatment response to drugs of this class. Following repeated treatment, initially sensitive lung tumors became resistant to Bortezomib. A second NF- κ B inhibitor, Bay-117082, showed similar therapeutic efficacy and acquired-resistance in mice. Our results using preclinical mouse models support the NF- κ B pathway as a potential therapeutic target for a defined subset of lung adenocarcinoma.

Significance:

By employing small molecule compounds that inhibit NF- κ B activity, we provide evidence that NF- κ B inhibition has therapeutic efficacy in the treatment of lung cancer. Our results also illustrate the value of mouse models to validate new drug targets *in vivo* and indicate that acquired chemoresistance may later influence Bortezomib treatment in lung cancer.

Introduction

Lung cancer is the leading cause of cancer death worldwide, with approximately 1.3 million people projected to die from this disease in the next year (1). Non-small cell lung cancer (NSCLC) represents 85% of lung cancer cases. Lung adenocarcinoma, a histological class of NSCLC, is associated with recurrent mutations in several well-defined oncogenes and tumor suppressor genes. Oncogenic *KRAS* mutations occur in approximately 25% of lung adenocarcinomas and inactivating mutations in the tumor suppressor gene p53 (*TP53*) are found in at least 50% of cases (1).

The 5-year survival rate of individuals diagnosed with lung cancer in the United States is poor at only ~15% and the prognosis is even worse for individuals diagnosed with advanced disease (2).

Although much effort has been devoted to developing targeted therapies for lung cancer, few such therapies have proven effective thus far (3). Recent successful targeted therapies include the EGFR inhibitor gefitinib/erlotinib for patients with *EGFR* mutation (4), and ALK (Anaplastic Lymphoma Kinase) inhibitors for patients with *EML4-ALK* translocations (5). Yet to date, no targeted therapies have been used effectively against *KRAS* mutant lung cancer.

The nuclear factor- κ B (NF- κ B) pathway is an emerging cancer drug target (6, 7). The mammalian NF- κ B transcription factor family is composed of five subunits: RELA (p65), RELB, REL (cRel), NF- κ B1 (p50 and its precursor p105) and NF- κ B2 (p52 and its precursor p100), which form homodimers or heterodimers (8). Two major NF- κ B pathways, canonical and alternative, have been well characterized (9). In the canonical pathway, NF- κ B (usually comprised of a p65-p50 heterodimer) is inhibited through sequestration in the cytoplasm by the inhibitor of κ B (I κ B) under non-stimulated conditions. I κ B is a target of several upstream signaling cascades that activate an I κ B kinase (IKK) complex composed of at least two kinases, IKK α and IKK β , and of one regulatory subunit, NF- κ B essential modulator (NEMO, also called IKK γ). Both IKK α and IKK β can directly phosphorylate I κ B, resulting in its ubiquitination and degradation by the 26S proteasome (7). Once released from I κ B, NF- κ B becomes active through nuclear translocation and DNA binding. In the alternative pathway, IKK α , activated by NF- κ B-inducing kinase (NIK), phosphorylates p100, resulting in limited degradation of p100 into p52 by the proteasome, followed by nuclear translocation of the RELB-p52 heterodimer (6).

The nuclear factor- κ B (NF- κ B) pathway has recently emerged as a promising cancer drug target (6, 7). NF- κ B transcriptional factors are crucial regulators of mechanisms associated with tumorigenesis, and their multifaceted function are achieved through regulation of NF- κ B target genes (6, 10). NF- κ B target genes are associated with numerous hallmarks of cancer (11), including inflammation (*TNF*, *IL6*, *IL1*, *ICAM1*, *MCPI*), proliferation (*MYC*, *CYCLIND1*,

CYCLINE2, *CDK2*), survival (*BCL2*, *BCLxL*, *cIAP1/2*, *XIAP*, *SURVIVIN*), tumor progression (*MMP2/9*, *COX2*), angiogenesis (*HIF1 α* , *VEGF*) and cell death (*FAS*, *FASL*). Because NF- κ B regulates a panel of key oncogenes (eg, *MYC*) and pro-survival genes (eg, *BCL2*), this pathway has also been implicated in tumor initiation, progression, and resistance to chemotherapy (12). Aberrant NF- κ B pathway activity has been frequently observed in human cancer through cancer genomic studies. For example, mutations in the NF- κ B pathway are detected in >20% of multiple myelomas (MM) (13), and are potentially involved in lung cancer (14). In diffuse large B-Cell lymphoma (DLBCL), NF- κ B mutations are found in >50% of the activated B-Cell-like (ABC) subtype but rarely in the germinal centre B-cell-like (GCB) subtype (15). Consistent with these observations, IKK inhibitors showed cytotoxicity selectively in ABC-DLBCL cell lines but not in GCB-DLBCL cells (16).

While small molecule compound inhibitors of NF- κ B have been proposed as rational single agent therapies for cancers with aberrant NF- κ B activity, most classical NF- κ B inhibitors are poorly selective and have known off-target effects (6, 17). Because proteasome-mediated degradation of I κ B is a required step in NF- κ B signaling, the proteasome inhibitor Bortezomib (Velcade/PS-341) has been proposed as a general inhibitor of NF- κ B (6, 7). Bortezomib is an FDA-approved first line treatment for advanced multiple myeloma, a disease with frequent NF- κ B-pathway activation (18-21). In multiple myeloma studies, patients with high NF- κ B are more sensitive to Bortezomib (22), suggesting that although proteasome inhibition may affect other signaling pathways, NF- κ B is an essential target of this drug (6). A second NF- κ B inhibitor, Bay-117082, was identified as a compound inhibiting cytokine-induced I κ B phosphorylation (23). Like Bortezomib, Bay-117082 has been shown to suppress NF- κ B signaling *in vitro* and *in vivo* (23, 24). This compound, though not clinically approved, has been studied in mouse lymphoma models (24).

Mouse models of human cancer are powerful tools to study tumor biology, genetics, and therapies. Previously, mouse models of Eμ-Myc B cell lymphoma were successfully used to study the chemotherapy response (25). Similar studies in mouse models of lung cancer have led to new insights into the activity of PI3K inhibitors (26) and cisplatin *in vivo* (2). Our laboratory has developed an autochthonous mouse model of human lung cancer, in which lung adenocarcinoma is initiated upon Cre recombinase-mediated activation of a $Kras^{G12D}$ allele. In this case, $Kras^{G12D}$ activation alone ($Kras^{LSL-G12D/wt}$, K model) generates low-grade adenocarcinomas (27). When combined with the concomitant loss of both p53 alleles ($Kras^{LSL-G12D/wt}; p53^{flax/flax}$, KP model), the mice develop lung tumors with a shorter latency and advanced histopathology (28, 29). These models are thus suitable to evaluate novel targeted small molecule compounds in a physiological setting.

We previously showed that activation of Kras and loss of p53 selectively activates NF-κB, and that genetic inhibition of the NF-κB pathway in tumor epithelial cells resulted in significantly delayed lung tumor progression (30). Similar genetic studies have showed that p65/RelA is required for $Kras^{G12D}$ induced lung tumorigenesis (31) and *Gprc5a* loss enhances NF-κB activation in lung epithelial cells and promotes tumorigenesis (32). These results indicate a critical function for NF-κB signaling in lung tumor development and suggest NF-κB inhibitory drugs as potential targeted therapies for lung cancers with mutations in Kras and p53 or with activation of the NF-κB pathway. Here we describe the short-term and long-term effects of two general NF-κB inhibitors, Bortezomib and Bay-117082, in the K and KP models of lung adenocarcinoma. The results indicate that small molecule inhibition of this pathway can cause tumor regression but that long-term treatment is associated with acquired resistance.

Materials and Methods.

Mice and drug treatment

The MIT Institutional Animal Care and Use Committee approved all animal studies and procedures. To initiate lung tumors, cohorts of K or KP mice of 129svJae background were infected with 2.5×10^7 plaque-forming units (PFU) of Adeno-Cre (University of Iowa) by intra-nasal inhalation as described previously (2, 28). Mice were given Bortezomib (LC Labs) in PBS (0.5% DMSO) at 1 mg/kg body weight intravenously (i.v.) as indicated. Bay-117082 (CalBiochem) was dissolved in DMSO, diluted in PBS as a fine suspension and injected at 10 mg/kg body weight intraperitoneally (i.p.) as indicated.

Immunohistochemistry

Mice were sacrificed by carbon dioxide asphyxiation. Lungs were inflated with 4% formalin (NBF), fixed overnight, and transferred to 70% ethanol. Lung lobes were embedded in paraffin and sectioned at 4 μ m and stained with hematoxylin and eosin (H&E) for tumor pathology. For staining with anti-cleaved caspase 3 antibodies (Cell Signaling #9661), lung tumor sections were de-waxed, rehydrated and subjected to high temperature antigen retrieval, 10 min boiling in a pressure cooker in 0.01 M citrate buffer pH 6.0. Slides were stained overnight at 4 degree in 1:100 primary antibody. A goat anti-rabbit HRP-conjugated secondary antibody (Vector Laboratories) was used at 1:200 dilution, incubated for 1 hours room temperature, followed by DAB staining (Vector Laboratories). The number of positive cells per tumor area was quantified using Bioquant software from >10 tumors in at least 3 mice per group (2).

MicroCT and bioluminescence imaging

At indicated time points, mice were scanned for 15 min under isoflurane anesthesia using a small animal eXplore Locus micro-computed tomography (microCT, GE Healthcare) at 45- μ m resolution, 80 kV, with 450-mA current (33). Images were acquired and processed using GE

eXplore software. Bioluminescence imaging was performed as previously described (34). Mice were imaged for 60 seconds and signals in the lung were quantified using Xenogen software.

Immunoblotting and immunofluorescence

Cell pellets were lysed in Laemmli buffer. Equal amounts of protein (16 μ g) were separated on 10% SDS-polyacrylamide gels and transferred to PVDF membranes. Blots were probed with antibodies (1:1000 dilution) against p65 (c-20), Nemo (FL-419), Parp (46D11), c-Rel (C), p100/p52 (Cell Signaling, #4882) or cleaved caspase 3 (Cell signaling #9661). Nuclear–cytoplasmic fractionations and NF- κ B p65 DNA-binding activity assay were as described recently (30). For NF- κ B subunits DNA-binding activity assay, five micrograms of nuclear extracts was used to determine NF- κ B DNA-binding activity anti-p65, p52, p50, RelB or C-Rel primary antibodies in an ELISA-based assay, according to the manufacturer's instructions (Active Motif TransAM). Immunofluorescence was performed as recently described (35). Antibodies are as following: p65 (c-20, 1:100), p100/p52 (Cell Signaling, #4882, 1:100) and goat-anti-rabbit Alexa-488 (Invitrogen, 1:1000). Cells were counterstained with 4, 6-diamidino-2-phenylindole (DAPI, Sigma) and mounted in Vectashield anti-fade mountant (Vector Laboratories, Burlingame, CA).

Cell viability assay

Cell culture conditions were as described recently (30). Cells were split into 96-well plates (5,000 cells per well). After 24 hours, cells were treated with Bortezomib, and 24 hours later cell viability was measured by Cell Titer Aqueous kit (Promega) in triplicates. Vehicle control treated cell values were set to 1 (100% viability). For Fig 2A and Fig S5A, the data are representative of two independent experiments.

Gene expression analysis

RNA was purified using Trizol (Invitrogen), according to the manufacturer's instructions. One microgram of RNA was reverse-transcribed using a High-Capacity cDNA Reverse Transcription Kit (Applied Biosystems). Real-time PCR (QPCR) amplification was performed using Taqman

probes (Applied Biosystems). Data were normalized to the *Gapdh* (mouse) or *GAPDH* (human) levels.

Statistics. P values were determined by Student's t-tests.

Results.

Bortezomib inhibits NF-κB signaling and induces apoptosis in lung adenocarcinoma cells.

Bortezomib has been shown to inhibit NF-κB by suppressing proteasome-mediated IκB degradation (19, 36). We thus hypothesized that Bortezomib would inhibit NF-κB signaling in lung adenocarcinoma cells. We have generated a panel of genetically-defined mouse lung adenocarcinoma cell lines (hereafter termed “KP”) from tumors carrying a Cre-activatable *Kras*^{G12D} allele (*Kras*^{LSL-G12D/WT}; LSL denotes Lox-stop-Lox) and a conditional loss-of-function p53 allele (*p53*^{flox/flox}). As shown in Figure 1A, Bortezomib-treated cells showed reduced nuclear accumulation of the NF-κB transcription factor subunit p65 (also known as RelA) compared to vehicle control treated cells. Because nuclear p65 is required for NF-κB activity, these data suggest that Bortezomib is able to inhibit the NF-κB pathway in mouse lung adenocarcinoma cells.

To explore the molecular and cellular effects of NF-κB inhibition in KP cells, we examined the expression levels of known NF-κB target genes by real-time PCR after a time course of Bortezomib treatment (Fig. 1B). Of note, NF-κB-regulated anti-apoptosis genes such as *Bcl2*, *Bclxl*, *Birc2* (*cIAP1*) and *Birc5* (*Survivin*) were consistently down-regulated at all time points tested, demonstrating the efficiency of NF-κB inhibition. Furthermore, proliferation-related NF-κB target genes including *c-Myc* and *Cyclin D1* also reduced expression following Bortezomib

treatment (Fig. 1B). Contrary to our expectations, the expression of three NF- κ B targets that regulate inflammation, *Il6*, *Tnf* and *Mmp3*, was not reduced after treatment and *Il6* messenger RNA level was actually increased in cells treated with Bortezomib. The induction of these inflammatory genes may be due to secondary effects of proteasome inhibition in these cells. Future experiments will examine the importance of Bortezomib's pro-inflammatory effects in tumor cells.

As the NF- κ B pathway is known to inhibit apoptosis through its regulation of anti-apoptotic genes, we next addressed the cytotoxicity of Bortezomib *in vitro*. (6). Consistent with decreased levels of *Bcl2* and other anti-apoptotic genes in Bortezomib-treated cells (Fig. 1B), we observed increased cleaved caspase 3 (CC3) in KP as well as in cells harboring the Kras^{G12D} mutation and a point mutation (R172H) in p53 (KP^M, T.G.O. and T.J., unpublished data) (37) (Fig. 1C). We also performed Trypan blue counting and confirmed that Bortezomib treatment caused cell death in a dose-dependent manner in KP and KP^M cells. Interestingly, LKR13 cells which express mutant Kras but retain wild-type p53 expression and 3TZ fibroblasts (30) did not show substantial cell death under the assayed conditions.

We also tested Bortezomib in two human NSCLC cell lines that contain mutations in *KRAS* and loss of function in *p53* (Fig. S1). Consistent with the mouse data, the NF- κ B target genes *MYC*, *BCL2* and *XIAP* were down-regulated in Bortezomib-treated human cells.

Bortezomib sensitivity correlates with basal NF- κ B activity in KP lung adenocarcinoma cells

To investigate the dose response profile of Bortezomib, we treated a panel of KP and KP^M cells with increasing doses of Bortezomib for 24 hours and monitored cell viability. As shown in

Figure 2A, KP and KP^M cell lines showed higher sensitivity to the drug than control 3TZ and *Kras*-only LKR13 cells. We previously showed that in KP cell lines, NF- κ B p65 DNA-binding activity was consistently higher than in 3TZ and LKR13 cells (30). By measuring NF- κ B target gene expression, we observed that KP and KP^M cells also have higher NF- κ B target gene expression than 3TZ or LKR13 cells (Fig. S2). To examine whether the level of NF- κ B activity might be a biomarker to predict Bortezomib response, we measured NF- κ B activity in KP cell lines using enzyme-linked immunosorbent assay (ELISA) (30) and quantified cell viability at 5 nM Bortezomib treatment. In the cell lines assayed, NF- κ B activity was positively correlated with Bortezomib induced cytotoxicity (Fig. 2B), with cell lines exhibiting high NF- κ B activity levels being more sensitive to the drug than cells with lower NF- κ B levels. Thus, we conclude that lung adenocarcinoma cells with high NF- κ B signaling are dependent on the continuous activation of this pathway. These data are consistent with studies showing multiple myelomas with high NF- κ B activity are more sensitive to Bortezomib (22) and IKK inhibitors (13).

Bortezomib leads to lung tumor regression in KP mice

Our cell based studies showed that Bortezomib induced apoptosis in murine lung adenocarcinoma cell lines grown in culture (Fig. 1C). To understand the relevance of these findings *in vivo*, we examined Bortezomib mediated NF- κ B inhibition in both the KP and K models of lung cancer. Previous data have shown that KP lung tumors have higher NF- κ B signaling than those from the K model (30). To test the functional requirement for NF- κ B in KP tumors, we infected 6-8 weeks old KP mice with adenoviruses expressing Cre (Adeno-Cre, Fig. S3A). 10 weeks after infection, mice were treated with a single dose of 1 mg/kg Bortezomib, a maximum tolerated dose that has been shown to inhibit the proteasome and NF- κ B activity in mice (19, 38). Individual lung tumors were monitored using microCT imaging prior to treatment (D0) and 4 days post treatment (D4). As shown in Figure 3A-B, a single dose of Bortezomib resulted in significant tumor regression

(55.4% average decrease in tumor volume at D4 compared to D0), whereas vehicle control treated mice showed a 47.2% average increase in tumor volume. Thus, established tumors with Kras mutations and loss of p53 function are acutely sensitive to treatment with Bortezomib.

To determine whether Bortezomib affects tumors from the K model, which retains functional p53, we initiated lung tumorigenesis in *Kras*^{LSL-G12D/wt} mice with Adeno-Cre and treated the mice with a single 1 mg/kg dose of Bortezomib at 20 weeks post infection (Fig. S3B). As shown in Figure 3C-D, K tumors did not regress upon Bortezomib treatment. Because tumors from KP mice had enhanced NF-κB p65 nuclear localization when compared to K tumors (30), the different therapeutic response between KP and K tumors suggests that the effect of Bortezomib may depend on the tumor genotype or the basal NF-κB activity.

To compare the efficacy of Bortezomib to other lung cancer therapies, we injected KP lung tumor cells subcutaneously into immune-compromised mice, allowed tumors to form and then treated the mice with Bortezomib. As shown in Figure S4, Bortezomib markedly reduced tumor volumes in the short term and diminished tumor progression to a similar extent as cisplatin, a first line chemotherapy for lung cancer (2).

Bortezomib induces apoptosis in KP lung tumors

To address the mechanism of Bortezomib-induced tumor regression, we stained control or Bortezomib-treated KP and K tumor sections with an antibody that recognizes cleaved caspase 3 (CC3). In KP tumors, we observed an increase in the number of apoptotic cells at 48 hours after a single dose of Bortezomib treatment (Fig. 4A). These results suggest that in the context of oncogenic Kras expression and p53 loss, Bortezomib treatment leads to apoptosis both *in vitro* (Fig. 1C) and *in vivo*. To investigate the kinetics of Bortezomib's effects *in vivo*, we stained

tumor sections derived from a time-course experiment with antibodies to CC3. As shown in Figure 4C, the CC3⁺ cell number peaked at 24 and 48 hrs post treatment and diminished at 96 hrs. This transient increase might be caused by the short half-life of Bortezomib *in vivo* (39).

Using a cohort of *Kras*^{LSL-G12D/wt} mice, we asked whether Bortezomib induces apoptosis in K-only tumors. In all the time points assayed, we did not detect a substantial number of apoptotic cells in Bortezomib-treated tumors (Fig. 4B, D). These results reinforced the importance of genetic context in the response to Bortezomib, and in particular the role of p53 mutation in conferring sensitivity to NF-κB inhibition.

Bortezomib increases survival in KP mice

To analyze the long-term effects of Bortezomib therapy, we investigated whether a four-dose regimen of Bortezomib (19) could prolong survival of tumor-bearing mice. Using a cohort of KP mice, we treated tumor-bearing animals 8 weeks following Adeno-Cre infection with Bortezomib once a week for 4 weeks (Fig. S3A). As shown in Figure 5A, KP mice treated with four doses of Bortezomib survived significantly longer (104.2±19.8 days) than control treated mice (76.8±10.6 days) (p=0.001). In contrast, consistent with the lack of tumor regression and cell death in *Kras*^{LSL-G12D/wt} mice observed after short term Bortezomib treatment (Fig. 3-4), there was no improvement in survival in the *Kras*^{LSL-G12D/wt} cohort (Fig. 5B, p=0.36). This suggests that loss of p53, while a predictor of poor prognosis in some cancer therapies, still permits therapeutic benefits from Bortezomib and indicates that Bortezomib and possibly other NF-κB inhibitors may work selectively in tumors with high basal NF-κB activity.

Acquired resistance arises in KP tumors after Bortezomib treatment

Although the four-dose regimen of Bortezomib prolonged survival in the KP lung tumor model, the treated mice eventually succumbed to their disease (Fig. 5A). To examine whether Bortezomib treated tumors relapse after repeated Bortezomib treatment, we treated another cohort of tumor bearing KP mice with Bortezomib once a week for 4 weeks. Tumor response was measured by twice weekly microCT to determine the volume of individual lung tumors. As we had observed with short-term microCT imaging (Fig 3A), Bortezomib treatment led to rapid KP tumor regression after the first dose (10.5 weeks, Fig. 5C) and delayed tumor growth compared to vehicle control. However, by the fourth dose (13 weeks, Fig. 5C), tumors had become insensitive to treatment, suggesting that they had acquired resistance to the drug.

To investigate whether KP tumors present at the end of the treatment regimen were resistant to Bortezomib-induced apoptosis, we treated KP mice as described above with three doses of Bortezomib or vehicle control. After an additional week, mice were treated with a final dose of Bortezomib and sacrificed 48 hours later. Tumors from mice that had received previous Bortezomib treatments no longer demonstrated significant CC3 staining in response to a final dose of the drug (Fig. 5D, right) when compared to acutely treated naïve tumors (Fig. 5D left). These data further suggest that the pretreated tumors had acquired resistance to Bortezomib.

An orthotopic lung tumor model for imaging response and resistance to Bortezomib

To facilitate imaging of Bortezomib treatment response, we adapted a transplantation-based orthotopic lung cancer mouse model (40). As outlined in Figure 6A, we infected KP cell lines with a retrovirus expressing firefly luciferase. The cells were transplanted into immunocompetent

recipient mice by intravenous injection, resulting in the development of *in situ* lung tumors that could be imaged and quantified by bioluminescence imaging.

To determine if Bortezomib therapy was effective in the orthotopic model, we transplanted 10,000 KP cells into host mice and treated the mice 5 weeks later either with control or 4 dose-regimen weekly Bortezomib (40). Similar to the autochthonous setting, Bortezomib treatment significantly increased survival in this model compared to the control-treated mice (average survival 47.0 ± 2.0 days for control and 64.0 ± 5.4 days for Bortezomib, $p = 1.4 \times 10^{-5}$, Fig. 6B). Bioluminescence imaging revealed a marked tumor regression at day 2 and day 4 post Bortezomib treatment (Fig. 6C), also reminiscent of the Bortezomib mediated lung tumor regression in the autochthonous model (Fig. 3A). After the second and third Bortezomib treatments, the lung tumor signal still decreased or stabilized. However, similar to the tumor relapse detected in the autochthonous model, a fourth dose of Bortezomib was ineffective (Fig. 6C), suggesting the relapsed tumors had become refractory to drug treatment.

To test if the onset of Bortezomib resistance was accompanied by increased NF- κ B activity, we generated cell lines from orthotopic KP tumors that were treated either with 4 doses of Bortezomib (resistant cell lines) or with vehicle controls (sensitive cell lines). As shown in Figure S5, resistant cells showed higher viability and increased colony formation compared to sensitive cells upon Bortezomib treatment (Fig. S5A, B). Importantly, when treated with Bortezomib in culture, resistant cells showed robust down-regulation of NF- κ B target genes regulating apoptosis and survival (Fig. S6), indicating Bortezomib was still effective in inhibiting the NF- κ B pathway. Sensitive and resistant cell lines were next used to evaluate the activity of both the canonical and non-canonical NF- κ B pathways. Immunoblots, ELISA and immunofluorescence analysis showed similar levels of cytoplasmic and nuclear NF- κ B subunits in the resistant and sensitive cells (Fig.

S7-S8). Moreover, transcriptional profiling of 10 NF- κ B target genes did not reveal a globally increased expression of NF- κ B targets in resistant tumor cells (Fig. S9). These data suggest that cells generated from Bortezomib-resistant lung tumors harbor similar levels of basal NF- κ B activity compared to sensitive cells.

The NF- κ B inhibitor Bay-117082 shows therapeutic efficacy *in vivo*

To expand the scope of pharmacological inhibition of NF- κ B, we next tested a compound that was developed as an inhibitor of IKK. IKK-mediated I κ B phosphorylation is required for I κ B degradation and NF- κ B activation (8), and Bay-117082 is a small molecule compound which inhibits this IKK kinase activity (23). Like Bortezomib, Bay-117082 has been shown to suppress NF- κ B signaling in cells and mice (23, 24). Unlike Bortezomib, which affects multiple cellular activities in addition to NF- κ B, the use of Bay-117082 provides an additional degree of selectivity for inhibiting this pathway.

We found that Bay-117082 treatment induced caspase 3 cleavage and cell death in KP cell lines *in vitro* (Fig. S10). We assessed the expression of the pro-survival NF- κ B target genes in these cells after Bay-117082 treatment and found that Bay-117082 down-regulates NF- κ B target genes such as *Bcl2*, *Bclxl* and *Xiap* (Fig. 7A). Next we tested Bay-117082 in our orthotopic lung tumor model (Fig. 7B). Using bioluminescence imaging, we observed that Bay-117082 treatment significantly reduced lung tumor signal in the initial phase (Fig. 7B, 0-9 days) and delayed lung tumor progression until 42 days (Fig. 7B). However, treated tumors eventually became refractory to therapy and progressed in the lung and distant organs despite continuous Bay-117082 treatment (see 42-63 days in Fig. 7B). These data suggest that the relapsed tumors acquired resistance to the drug.

Finally, to gain insight into the survival benefit of Bay-117082, we treated a cohort of KP mice (8 weeks post Adeno-Cre) with three times weekly Bay-117082 (10 mg/kg) by intraperitoneal injection (i.p.) for four weeks, a dose previously shown to inhibit NF- κ B in mice (24). As shown in Fig. 7C, the KP mice treated with Bay-117082 survived significantly longer than mice treated with vehicle control (79.0 ± 13.2 days for control and 120.2 ± 27.0 days for Bay-117082, $p=0.008$). In a short-term treatment, BAY-117082 led to apoptosis, as indicated by cleavage of caspase 3 (Fig. S11). Altogether, these results indicate that IKK inhibition has therapeutic efficacy in lung cancer.

Discussion.

The NF- κ B pathway has recently emerged as a promising cancer therapeutic target (7). Large-scale RNAi screens and mouse model studies have documented that components of the NF- κ B signaling pathway are required for the survival of lung cancer cells and other cancer cell types (30, 41). Our study evaluated the efficacy of pharmacologically targeting NF- κ B in lung cancer. Our data showed that Bortezomib, used as a single agent, provided significant survival advantage in a KRas^{G12D}-driven p53-deficient lung cancer model. Bay-117082, an IKK inhibitory compound, also provided a survival advantage, although at a more frequent dosing schedule than the Bortezomib regimen. Our study provides proof that the NF- κ B pathway is a potential therapeutic target in lung cancer, and with further characterization of NF- κ B genetic mutations and NF- κ B target gene expression profiling in these types of tumors, treatment with NF- κ B inhibitors may become an important option for lung cancer targeted therapy.

Our study highlights the value of mouse models to translate genetic knowledge into novel and improved cancer therapies. Our autochthonous model not only recapitulates important genetic and

pathological features of human lung adenocarcinoma, but also provides a physiological tumor microenvironment to study therapeutic response. The orthotopic model, a variant of this approach, is based on the isolation of mouse lung adenocarcinoma cells from genetically tractable primary mouse lung tumors, followed by their seeding into the lungs of immunocompetent recipient mice (40). This latter model is also important for its ability to accelerate cancer treatment studies in mice, by allowing rapid imaging of therapeutic response and *ex vivo* genetic modification of cells by introduction of short hairpin RNAs or cDNAs. Using both systems, we have shown that mouse models, when combined with *in vivo* imaging and tumor biomarker analysis, can serve as a powerful platform to identify and validate novel cancer therapies. These mouse models will provide valuable preclinical information to be cross-compared to clinical trial data in human patients. Such studies could potentially dissect molecular mechanisms of selected drugs and identify biomarkers to predict patient response.

We have shown that Bortezomib treatment induced apoptosis in lung tumors driven by activated Kras and lacking p53. Apoptosis may be one of the mechanisms underlying the significant decrease in lung tumor burden by this drug in the KP model. We performed molecular characterization in cultured KP cells to show that Bortezomib reduced expression of anti-apoptotic NF- κ B target genes (eg, *Bcl2*, *Bclxl*, *Birc2*, *Xiap*, Fig. 1B). This result is consistent with a pro-survival function of NF- κ B in normal and cancer cells (8). Previous studies have developed inhibitors for Bcl2 family proteins (ABT-737) (42) and cIAP1 (43, 44) as novel cancer therapies, but considering the simultaneous suppression of many anti-apoptotic genes observed in Bortezomib treated cells (Fig. 1B), NF- κ B inhibition appears to provide a promising approach to lower the apoptosis threshold in cancer cells. Because human tumors often up-regulate NF- κ B signaling to gain resistance to chemotherapy (12), NF- κ B inhibitors may also serve as chemosensitizing agents in combination therapies.

Of note, Bortezomib and Bay-117082 have differential effects in the transcriptional profile of certain NF- κ B targets *in vitro*. For example, Bcl2 and Myc inhibition was more robust upon Bortezomib treatment, whereas Xiap inhibition was stronger upon Bay-117082 treatment (Fig. 1B and Fig. 7A). Although Bay-117082 treated mice survived slightly longer than Bortezomib treated cohort, these two groups were not statistically significant ($p=0.103$), and this effect may be due to a more frequent dosing schedule of Bay-117082 (3 injections per week) than Bortezomib. Our treatment data suggested that the efficacy of Bortezomib is dependent on the genetic context of lung tumors. Our previous study showed that genetic inhibition of NF- κ B by a I κ B super-repressor (a dominant negative form of I κ B) or knockdown of p65/RelA or Nemo preferentially triggered cell death in KP cells but not in 3TZ or LKR13 cells (30). In this treatment study, KP cells also showed greater Bortezomib sensitivity than 3TZ or Kras-only cells. *In vivo*, KP tumors with high NF- κ B activity were sensitive to Bortezomib whereas Kras-only tumors with lower activity were not responsive, which is consistent with clinical data that a NF- κ B signature in multiple myeloma patients is associated with better treatment outcome of Bortezomib (22). Phase II clinical trials indicated that Bortezomib has modest effects in advanced NSCLC patients previously treated with chemotherapy (45). Our observations that Bortezomib sensitivity correlates with NF- κ B activity suggest that NF- κ B is a major target of this drug and NF- κ B pathway activity may serve as a biomarker to predict the therapeutic response of Bortezomib or other NF- κ B inhibitory drugs.

In addition to inhibiting NF- κ B, Bortezomib and Bay-117082 have known multi-targeted effects. Bortezomib can also stabilize the CDK inhibitors p21 and p27 (46), while Bay-117082 can stimulate the stress-activated protein kinases, p38 and JNK-1 (23). New classes of more selective NF- κ B inhibitors such as ATP analog IKK inhibitors will improve efforts to drug the NF- κ B pathway in cancer. Moreover, the therapeutic inhibition of NF- κ B has thus far been viewed with caution due to this pathway's diverse functions in different physiological contexts such as the

immune system. Despite these cautions, Bortezomib has been extensively used in the clinic with manageable side effects. Future work will be required to address the safety profile of Bay-117082 or related molecules and their impact on non-cancerous tissue.

We further observed that prolonged Bortezomib treatment led to resistance in KP lung tumors. Acquired Bortezomib resistance has been reported in the literature (47), and our results are in agreement with clinical findings that multiple myelomas initially responsive to Bortezomib often relapse and become resistant to the drug (47). Several studies have suggested possible mechanisms of Bortezomib resistance, such as: (i) mutations or over-expression of the PSMB5 subunit of 26S proteasome (48) (ii) over-expression of HSP27 (49) and (iii) increased activity of the aggresome pathway (47). Interestingly, basal NF- κ B activity is not increased in Bortezomib-resistant lung tumor cell lines at least *in vitro* (Fig. S5-S9). Our studies establish a physiologically relevant system to explore the mechanisms of Bortezomib resistance in lung cancer.

In summary, we have characterized the therapeutic response and resistance to NF- κ B inhibitors in several mouse models of lung cancer. *In vivo* treatment with Bortezomib or Bay-117082 significantly reduced tumor volume and increased survival in mouse lung tumors associated with high NF- κ B activity. However, repeated treatment resulted in the emergence of drug resistance tumors, which may recapitulate important features that will occur in human patients. Mouse models will undoubtedly be useful for studying additional NF- κ B inhibitors as well as combination therapies.

Acknowledgements We thank D. McFadden, M. DuPage, A. Dooley, N. Joshi, N. Dimitrova, K. Lane, and E. Snyder for discussions and for sharing various reagents, A. Deconinck and C. Kim for critical reading of the manuscript, D. Crowley for preparation of tissue sections, S. Malstrom for animal imaging, and G. Mulligan at Millennium Pharmaceuticals and the entire Jacks laboratory for discussions. This work was supported by the Howard Hughes Medical Institute

(T.J.) and partially by a Cancer Center Support grant from the NCI (P30-CA14051). T.J. is the David H. Koch Professor of Biology and a Daniel K. Ludwig Scholar. W.X. is a recipient of fellowships from the American Association for Cancer Research and the Leukemia & Lymphoma Society. E.M. is a recipient of a fellowship from the International Human Frontier Science Program Organization. T.G.O. is an ASPETMerck postdoctoral fellow and supported by a Ludwig Fund postdoctoral fellowship. D.M.F. is a recipient of a Leukemia & Lymphoma Society Fellow Award. M.M.W. is a recipient of a Damon Runyon Cancer Research Foundation Merck Fellowship and a Genentech Postdoctoral Fellowship.

Figure Legends:

Figure 1. Bortezomib inhibits NF- κ B signaling and induces apoptosis in murine lung adenocarcinoma cell lines. (A) Bortezomib reduces nuclear p65 level. Two KP (*Kras*^{LSL-G12D/wt}; *p53*^{flox/flox}) cell lines (KP1 and KP2) were treated with 5nM Bortezomib (BZ) or vehicle control (ctrl) for 24 hours. Nuclear (N) and cytoplasmic (C) fractions of protein lysates were immunoblotted with the indicated antibodies. Nemo and Parp serve as cytoplasmic and nuclear loading controls respectively. (B) QPCR analysis of a subset of NF- κ B target genes in 5nM Bortezomib (BZ) treated KP cells at the indicated time points. Vehicle control is set to 1. (C) Bortezomib induces apoptosis in KP and KP^M (*Kras*^{LSL-G12D/wt}; *p53*^{R127H/-}) cells. Cells were treated with 5nM Bortezomib for 24 hours and protein lysates were immunoblotted with cleaved caspase 3 (CC3) and Tubulin antibodies. D, Quantification of cell death in Bortezomib treated cells. Cells were treated with the indicated concentrations of Bortezomib for 24 hours and dead cells were quantified by Trypan blue staining. Error bars are s.d. (n=3).

Figure 2. Bortezomib sensitivity correlates with basal NF- κ B activity in KP lung adenocarcinoma cell lines. (A) Relative cell viability in cell lines treated with increasing doses of Bortezomib for 24 hours. 3TZ, diamond; LKR13, triangle; KP, solid lines; KP^M, dashed lines. Error bars are s.d. (n=3). (B) Lung cancer cell lines with high basal NF- κ B activity were sensitive to Bortezomib. NF- κ B p65 DNA binding activity was determined by ELISA from nuclear extracts of KP cell lines and LKR13 cells (set as 1). Relative viability was measured after 5nM Bortezomib treatment as in (A).

Figure 3. Bortezomib induces acute lung tumor regression in *Kras*^{LSL-G12D/wt}; *p53*^{flox/flox} (KP) but not in *Kras*^{LSL-G12D/wt} (K) mice. (A,C) Representative microCT images (n=6) of KP (A) and K (C) lung tumors prior to treatment (D0) and 4 days (D4) after a single dose of vehicle control

or Bortezomib. **(B,D)**, Quantification of tumor volume change (D4 compared to D0) in control and Bortezomib treated mice. Each bar represents an individual tumor. $p < 10^{-6}$ in KP mice (B), $p > 0.05$ in K mice (D).

Figure 4. Bortezomib induces apoptosis in KP lung tumors. (A-B), H&E and cleaved caspase 3 (CC3) immunohistochemistry staining (200x) in vehicle control and Bortezomib treated KP (A) and K (B) lung tumors. **(C-D)** Quantification of CC3 positive cells in Bortezomib treated KP (C) and K (D) lung tumors at indicated time points. “0 hour” represents vehicle control treated tumors. Error bars are s.d. ($n > 10$ for each time point).

Figure 5. Bortezomib increases survival in KP mice. (A-B), Kaplan-Meier survival curve of vehicle control and Bortezomib treated KP (A) and K (B) mice. Arrows indicate weekly 1mg/kg Bortezomib regimen. **(C)** Quantification of lung tumor volume of control and Bortezomib treated KP mice. From 10 weeks post Adeno-Cre infection, lungs were imaged by microCT to measure individual tumour volumes ($n = 4$). Data points represent means of fold change and s.d. relative to 10 weeks (set to 1). Arrows indicate Bortezomib injection. **(D)** Cleaved caspase 3 (CC3) staining (200x) in lung tumors receiving 3 doses of control (“C”) and 1 final dose of Bortezomib (“B”) (left) or 4 doses of Bortezomib (right). Tumors were harvested 48 hours after the last treatment ($n = 4$).

Figure 6. Imaging Bortezomib response and resistance in an orthotopic lung tumor model. (A) Experimental design. Lung cancer cells derived from KP tumors were infected with a retrovirus expressing luciferase and transplanted into immunocompetent recipient mice by tail vein injection. **(B)** Kaplan-Meier survival curve of control and Bortezomib treated recipient mice ($n = 6$, $p = 1.4 \times 10^{-5}$). 10,000 cells were transplanted and treatment started after 35 days. **(C)** Representative bioluminescence imaging of recipient mice ($n = 6$) treated with vehicle control or Bortezomib as in (B). D0 refers to the first treatment. Arrows indicate weekly Bortezomib regimen.

Figure 7. The NF- κ B inhibitor Bay-117082 leads to lung tumor regression *in vivo*. (A) QPCR analysis of NF- κ B target gene expression in KP cells treated with 10 μ M Bay-117082 for indicated hours (hr). Error bars are s.d. ($n = 3$). **(B)** Bay-117082 treatment leads to lung tumor regression and delays tumor progression in the orthotopic lung tumor model. 50,000 luciferase tagged KP cells were transplanted into recipient mice ($n = 6$) and treatment started at 19 days post transplantation (set at D0). Mice were treated with vehicle control or 10mg/kg Bay-117082 by i.p. injection, and imaged at the indicated time points. Arrows indicate Bay-117082 injections. **(C)**

Bay-**117082** prolongs survival in the KP model (n=6, p=0.008). “i.p. dosing” indicates 3 doses per week treatment.

Reference List

- 1 Herbst,R.S., Heymach,J.V. and Lippman,S.M. Lung cancer, *N.Engl.J.Med.*, 359: 1367-1380, 2008.
- 2 Oliver,T.G., Mercer,K.L., Sayles,L.C., Burke,J.R., Mendus,D., Lovejoy,K.S., Cheng,M.H., Subramanian,A., Mu,D., Powers,S., Crowley,D., Bronson,R.T., Whittaker,C.A., Bhutkar,A., Lippard,S.J., Golub,T., Thomale,J., Jacks,T. and Sweet-Cordero,E.A. Chronic cisplatin treatment promotes enhanced damage repair and tumor progression in a mouse model of lung cancer, *Genes Dev.*, 24: 837-852, 2010.
- 3 Downward,J. Targeting RAS signalling pathways in cancer therapy, *Nat.Rev.Cancer*, 3: 11-22, 2003.
- 4 Sordella,R., Bell,D.W., Haber,D.A. and Settleman,J. Gefitinib-sensitizing EGFR mutations in lung cancer activate anti-apoptotic pathways, *Science*, 305: 1163-1167, 2004.
- 5 Gerber,D.E. and Minna,J.D. ALK inhibition for non-small cell lung cancer: from discovery to therapy in record time, *Cancer Cell*, 18: 548-551, 2010.
- 6 Baud,V. and Karin,M. Is NF-kappaB a good target for cancer therapy? Hopes and pitfalls, *Nat.Rev.Drug Discov.*, 8: 33-40, 2009.
- 7 Karin,M., Yamamoto,Y. and Wang,Q.M. The IKK NF-kappa B system: a treasure trove for drug development, *Nat.Rev.Drug Discov.*, 3: 17-26, 2004.
- 8 Hayden,M.S. and Ghosh,S. Signaling to NF-kappaB, *Genes Dev.*, 18: 2195-2224, 2004.
- 9 Baltimore,D. Discovering NF-kappaB, *Cold Spring Harb.Perspect.Biol.*, 1: a000026, 2009.
- 10 Basseres,D.S. and Baldwin,A.S. Nuclear factor-kappaB and inhibitor of kappaB kinase pathways in oncogenic initiation and progression, *Oncogene*, 25: 6817-6830, 2006.
- 11 Hanahan,D. and Weinberg,R.A. The hallmarks of cancer, *Cell*, 100: 57-70, 2000.

- 12 Nakanishi,C. and Toi,M. Nuclear factor-kappaB inhibitors as sensitizers to anticancer drugs, *Nat.Rev.Cancer*, 5: 297-309, 2005.
- 13 Annunziata,C.M., Davis,R.E., Demchenko,Y., Bellamy,W., Gabrea,A., Zhan,F., Lenz,G., Hanamura,I., Wright,G., Xiao,W., Dave,S., Hurt,E.M., Tan,B., Zhao,H., Stephens,O., Santra,M., Williams,D.R., Dang,L., Barlogie,B., Shaughnessy,J.D., Jr., Kuehl,W.M. and Staudt,L.M. Frequent engagement of the classical and alternative NF-kappaB pathways by diverse genetic abnormalities in multiple myeloma, *Cancer Cell*, 12: 115-130, 2007.
- 14 Kan,Z., Jaiswal,B.S., Stinson,J., Janakiraman,V., Bhatt,D., Stern,H.M., Yue,P., Haverty,P.M., Bourgon,R., Zheng,J., Moorhead,M., Chaudhuri,S., Tomsho,L.P., Peters,B.A., Pujara,K., Cordes,S., Davis,D.P., Carlton,V.E., Yuan,W., Li,L., Wang,W., Eigenbrot,C., Kaminker,J.S., Eberhard,D.A., Waring,P., Schuster,S.C., Modrusan,Z., Zhang,Z., Stokoe,D., de Sauvage,F.J., Faham,M. and Seshagiri,S. Diverse somatic mutation patterns and pathway alterations in human cancers, *Nature*, 466: 869-873, 2010.
- 15 Compagno,M., Lim,W.K., Grunn,A., Nandula,S.V., Brahmachary,M., Shen,Q., Bertoni,F., Ponzoni,M., Scandurra,M., Califano,A., Bhagat,G., Chadburn,A., la-Favera,R. and Pasqualucci,L. Mutations of multiple genes cause deregulation of NF-kappaB in diffuse large B-cell lymphoma, *Nature*, 459: 717-721, 2009.
- 16 Lam,L.T., Davis,R.E., Pierce,J., Hepperle,M., Xu,Y., Hottelet,M., Nong,Y., Wen,D., Adams,J., Dang,L. and Staudt,L.M. Small molecule inhibitors of IkappaB kinase are selectively toxic for subgroups of diffuse large B-cell lymphoma defined by gene expression profiling, *Clin.Cancer Res.*, 11: 28-40, 2005.
- 17 Gilmore,T.D. and Herscovitch,M. Inhibitors of NF-kappaB signaling: 785 and counting, *Oncogene*, 25: 6887-6899, 2006.
- 18 Chauhan,D., Hideshima,T. and Anderson,K.C. Proteasome inhibition in multiple myeloma: therapeutic implication, *Annu.Rev.Pharmacol.Toxicol.*, 45: 465-476, 2005.
- 19 Adams,J., Palombella,V.J., Sausville,E.A., Johnson,J., Destree,A., Lazarus,D.D., Maas,J., Pien,C.S., Prakash,S. and Elliott,P.J. Proteasome inhibitors: a novel class of potent and effective antitumor agents, *Cancer Res.*, 59: 2615-2622, 1999.

- 20 LeBlanc,R., Catley,L.P., Hideshima,T., Lentzsch,S., Mitsiades,C.S., Mitsiades,N., Neuberg,D., Goloubeva,O., Pien,C.S., Adams,J., Gupta,D., Richardson,P.G., Munshi,N.C. and Anderson,K.C. Proteasome inhibitor PS-341 inhibits human myeloma cell growth in vivo and prolongs survival in a murine model, *Cancer Res.*, 62: 4996-5000, 2002.
- 21 Richardson,P.G., Mitsiades,C., Hideshima,T. and Anderson,K.C. Bortezomib: proteasome inhibition as an effective anticancer therapy, *Annu.Rev.Med.*, 57: 33-47, 2006.
- 22 Mulligan,G., Mitsiades,C., Bryant,B., Zhan,F., Chng,W.J., Roels,S., Koenig,E., Fergus,A., Huang,Y., Richardson,P., Trepicchio,W.L., Broyl,A., Sonneveld,P., Shaughnessy,J.D., Jr., Bergsagel,P.L., Schenkein,D., Esseltine,D.L., Boral,A. and Anderson,K.C. Gene expression profiling and correlation with outcome in clinical trials of the proteasome inhibitor bortezomib, *Blood*, 109: 3177-3188, 2007.
- 23 Pierce,J.W., Schoenleber,R., Jesmok,G., Best,J., Moore,S.A., Collins,T. and Gerritsen,M.E. Novel inhibitors of cytokine-induced IkappaBalpha phosphorylation and endothelial cell adhesion molecule expression show anti-inflammatory effects in vivo, *J.Biol.Chem.*, 272: 21096-21103, 1997.
- 24 Keller,S.A., Hernandez-Hopkins,D., Vider,J., Ponomarev,V., Hyjek,E., Schattner,E.J. and Cesarman,E. NF-kappaB is essential for the progression of KSHV- and EBV-infected lymphomas in vivo, *Blood*, 107: 3295-3302, 2006.
- 25 Schmitt,C.A., Fridman,J.S., Yang,M., Lee,S., Baranov,E., Hoffman,R.M. and Lowe,S.W. A senescence program controlled by p53 and p16INK4a contributes to the outcome of cancer therapy, *Cell*, 109: 335-346, 2002.
- 26 Engelman,J.A., Chen,L., Tan,X., Crosby,K., Guimaraes,A.R., Upadhyay,R., Maira,M., McNamara,K., Perera,S.A., Song,Y., Chirieac,L.R., Kaur,R., Lightbown,A., Simendinger,J., Li,T., Padera,R.F., Garcia-Echeverria,C., Weissleder,R., Mahmood,U., Cantley,L.C. and Wong,K.K. Effective use of PI3K and MEK inhibitors to treat mutant Kras G12D and PIK3CA H1047R murine lung cancers, *Nat.Med.*, 14: 1351-1356, 2008.
- 27 Jackson,E.L., Willis,N., Mercer,K., Bronson,R.T., Crowley,D., Montoya,R., Jacks,T. and Tuveson,D.A. Analysis of lung tumor initiation and progression using conditional expression of oncogenic K-ras, *Genes Dev.*, 15: 3243-3248, 2001.

- 28 DuPage,M., Dooley,A.L. and Jacks,T. Conditional mouse lung cancer models using adenoviral or lentiviral delivery of Cre recombinase, *Nat.Protoc.*, 4: 1064-1072, 2009.
- 29 Tuveson,D.A., Shaw,A.T., Willis,N.A., Silver,D.P., Jackson,E.L., Chang,S., Mercer,K.L., Grochow,R., Hock,H., Crowley,D., Hingorani,S.R., Zaks,T., King,C., Jacobetz,M.A., Wang,L., Bronson,R.T., Orkin,S.H., DePinho,R.A. and Jacks,T. Endogenous oncogenic K-ras(G12D) stimulates proliferation and widespread neoplastic and developmental defects, *Cancer Cell*, 5: 375-387, 2004.
- 30 Meylan,E., Dooley,A.L., Feldser,D.M., Shen,L., Turk,E., Ouyang,C. and Jacks,T. Requirement for NF-kappaB signalling in a mouse model of lung adenocarcinoma, *Nature*, 462: 104-107, 2009.
- 31 Basseres,D.S., Ebbs,A., Levantini,E. and Baldwin,A.S. Requirement of the NF-kappaB subunit p65/RelA for K-Ras-induced lung tumorigenesis, *Cancer Res.*, 70: 3537-3546, 2010.
- 32 Deng,J., Fujimoto,J., Ye,X.F., Men,T.Y., Van Pelt,C.S., Chen,Y.L., Lin,X.F., Kadara,H., Tao,Q., Lotan,D. and Lotan,R. Knockout of the tumor suppressor gene Gprc5a in mice leads to NF-kappaB activation in airway epithelium and promotes lung inflammation and tumorigenesis, *Cancer Prev.Res.(Phila)*, 3: 424-437, 2010.
- 33 Kirsch,D.G., Grimm,J., Guimaraes,A.R., Wojtkiewicz,G.R., Perez,B.A., Santiago,P.M., Anthony,N.K., Forbes,T., Doppke,K., Weissleder,R. and Jacks,T. Imaging primary lung cancers in mice to study radiation biology, *Int.J.Radiat.Oncol.Biol.Phys.*, 76: 973-977, 2010.
- 34 Xue,W., Krasnitz,A., Lucito,R., Sordella,R., Vanaelst,L., Cordon-Cardo,C., Singer,S., Kuehnel,F., Wigler,M., Powers,S., Zender,L. and Lowe,S.W. DLC1 is a chromosome 8p tumor suppressor whose loss promotes hepatocellular carcinoma, *Genes Dev.*, 22: 1439-1444, 2008.
- 35 Zender,L., Xue,W., Zuber,J., Semighini,C.P., Krasnitz,A., Ma,B., Zender,P., Kubicka,S., Luk,J.M., Schirmacher,P., McCombie,W.R., Wigler,M., Hicks,J., Hannon,G.J., Powers,S. and Lowe,S.W. An oncogenomics-based in vivo RNAi screen identifies tumor suppressors in liver cancer, *Cell*, 135: 852-864, 2008.
- 36 Hideshima,T., Richardson,P., Chauhan,D., Palombella,V.J., Elliott,P.J., Adams,J. and Anderson,K.C. The proteasome inhibitor PS-341 inhibits growth, induces apoptosis, and

- overcomes drug resistance in human multiple myeloma cells, *Cancer Res.*, *61*: 3071-3076, 2001.
- 37 Jackson,E.L., Olive,K.P., Tuveson,D.A., Bronson,R., Crowley,D., Brown,M. and Jacks,T.
The differential effects of mutant p53 alleles on advanced murine lung cancer, *Cancer Res.*, *65*: 10280-10288, 2005.
 - 38 Sunwoo,J.B., Chen,Z., Dong,G., Yeh,N., Crowl,B.C., Sausville,E., Adams,J., Elliott,P. and Van,W.C. Novel proteasome inhibitor PS-341 inhibits activation of nuclear factor-kappa B, cell survival, tumor growth, and angiogenesis in squamous cell carcinoma, *Clin.Cancer Res.*, *7*: 1419-1428, 2001.
 - 39 Dubey,S. and Schiller,J.H. Three emerging new drugs for NSCLC: pemetrexed, bortezomib, and cetuximab, *Oncologist.*, *10*: 282-291, 2005.
 - 40 Doles,J., Oliver,T.G., Cameron,E.R., Hsu,G., Jacks,T., Walker,G.C. and Hemann,M.T.
Suppression of Rev3, the catalytic subunit of Pol{zeta}, sensitizes drug-resistant lung tumors to chemotherapy, *Proc.Natl.Acad.Sci.U.S.A.*, *107*: 20786-20791, 2010.
 - 41 Barbie,D.A., Tamayo,P., Boehm,J.S., Kim,S.Y., Moody,S.E., Dunn,I.F., Schinzel,A.C., Sandy,P., Meylan,E., Scholl,C., Frohling,S., Chan,E.M., Sos,M.L., Michel,K., Mermel,C., Silver,S.J., Weir,B.A., Reiling,J.H., Sheng,Q., Gupta,P.B., Wadlow,R.C., Le,H., Hoersch,S., Wittner,B.S., Ramaswamy,S., Livingston,D.M., Sabatini,D.M., Meyerson,M., Thomas,R.K., Lander,E.S., Mesirov,J.P., Root,D.E., Gilliland,D.G., Jacks,T. and Hahn,W.C. Systematic RNA interference reveals that oncogenic KRAS-driven cancers require TBK1, *Nature*, *462*: 108-112, 2009.
 - 42 Oltsersdorf,T., Elmore,S.W., Shoemaker,A.R., Armstrong,R.C., Augeri,D.J., Belli,B.A., Bruncko,M., Deckwerth,T.L., Dinges,J., Hajduk,P.J., Joseph,M.K., Kitada,S., Korsmeyer,S.J., Kunzer,A.R., Letai,A., Li,C., Mitten,M.J., Nettesheim,D.G., Ng,S., Nimmer,P.M., O'Connor,J.M., Oleksijew,A., Petros,A.M., Reed,J.C., Shen,W., Tahir,S.K., Thompson,C.B., Tomaselli,K.J., Wang,B., Wendt,M.D., Zhang,H., Fesik,S.W. and Rosenberg,S.H. An inhibitor of Bcl-2 family proteins induces regression of solid tumours, *Nature*, *435*: 677-681, 2005.
 - 43 Varfolomeev,E., Blankenship,J.W., Wayson,S.M., Fedorova,A.V., Kayagaki,N., Garg,P., Zobel,K., Dynek,J.N., Elliott,L.O., Wallweber,H.J., Flygare,J.A., Fairbrother,W.J., Deshayes,K., Dixit,V.M. and Vucic,D. IAP antagonists induce autoubiquitination of c-IAPs, NF-kappaB activation, and TNFalpha-dependent apoptosis, *Cell*, *131*: 669-681, 2007.
 - 44 Vince,J.E., Wong,W.W., Khan,N., Feltham,R., Chau,D., Ahmed,A.U., Benetatos,C.A., Chunduru,S.K., Condon,S.M., McKinlay,M., Brink,R., Leverkus,M., Tergaonkar,V.,

- Schneider,P., Callus,B.A., Koentgen,F., Vaux,D.L. and Silke,J. IAP antagonists target cIAP1 to induce TNFalpha-dependent apoptosis, *Cell*, *131*: 682-693, 2007.
- 45 Fanucchi,M.P., Fossella,F.V., Belt,R., Natale,R., Fidias,P., Carbone,D.P., Govindan,R., Racz,L.E., Robert,F., Ribeiro,M., Akerley,W., Kelly,K., Limentani,S.A., Crawford,J., Reimers,H.J., Axelrod,R., Kashala,O., Sheng,S. and Schiller,J.H. Randomized phase II study of bortezomib alone and bortezomib in combination with docetaxel in previously treated advanced non-small-cell lung cancer, *J.Clin.Oncol.*, *24*: 5025-5033, 2006.
- 46 Mack,P.C., Davies,A.M., Lara,P.N., Gumerlock,P.H. and Gandara,D.R. Integration of the proteasome inhibitor PS-341 (Velcade) into the therapeutic approach to lung cancer, *Lung Cancer*, *41 Suppl 1*: S89-S96, 2003.
- 47 Kumar,S. and Rajkumar,S.V. Many facets of bortezomib resistance/susceptibility, *Blood*, *112*: 2177-2178, 2008.
- 48 Oerlemans,R., Franke,N.E., Assaraf,Y.G., Cloos,J., van,Z., I, Berkers,C.R., Scheffer,G.L., Debipersad,K., Vojtekova,K., Lemos,C., van der Heijden,J.W., Ylstra,B., Peters,G.J., Kaspers,G.L., Dijkmans,B.A., Scheper,R.J. and Jansen,G. Molecular basis of bortezomib resistance: proteasome subunit beta5 (PSMB5) gene mutation and overexpression of PSMB5 protein, *Blood*, *112*: 2489-2499, 2008.
- 49 Chauhan,D., Li,G., Shringarpure,R., Podar,K., Ohtake,Y., Hideshima,T. and Anderson,K.C. Blockade of Hsp27 overcomes Bortezomib/proteasome inhibitor PS-341 resistance in lymphoma cells, *Cancer Res.*, *63*: 6174-6177, 2003.

Fig. 1

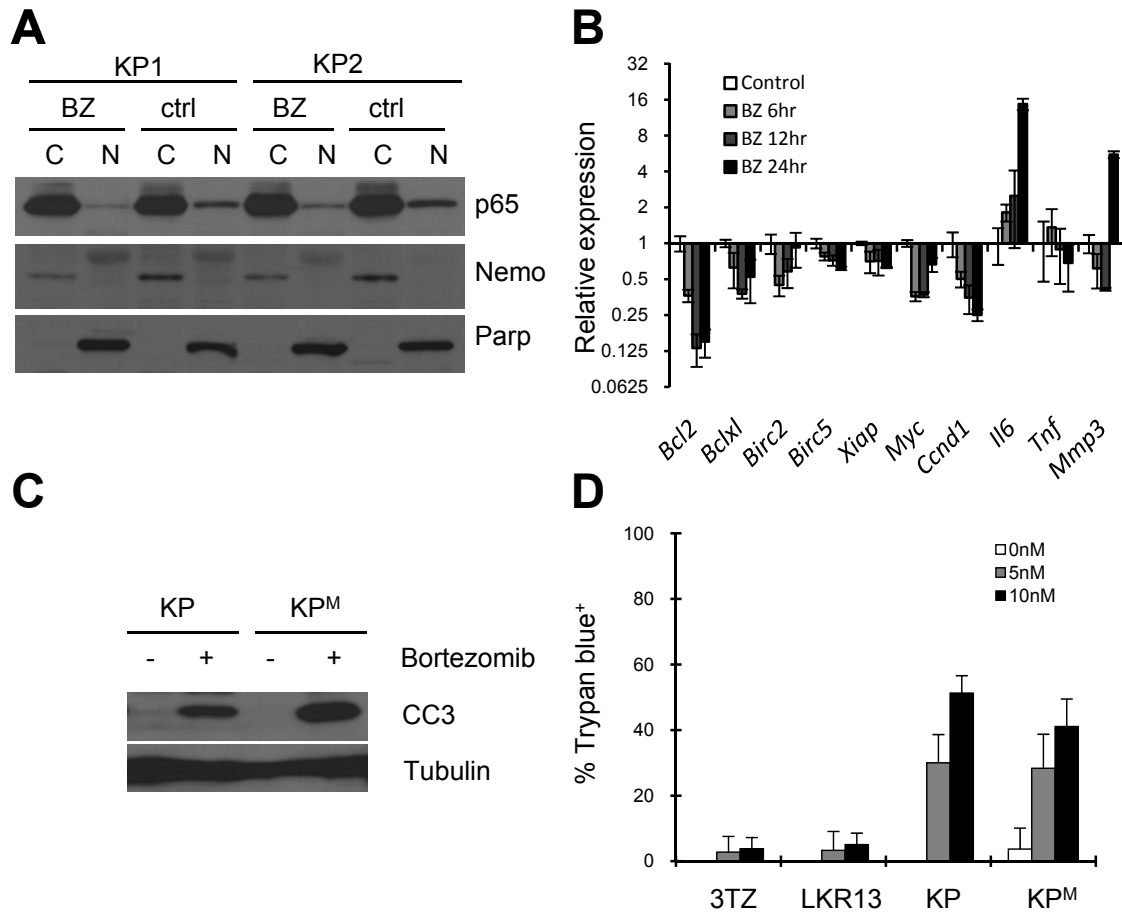


Figure 1. Bortezomib inhibits NF- κ B signaling and induces apoptosis in murine lung adenocarcinoma cell lines. (A) Bortezomib reduces nuclear p65 level. Two KP (*Kras*^{LSL-G12D/wt}; *p53*^{flox/flox}) cell lines (KP1 and KP2) were treated with 5nM Bortezomib (BZ) or vehicle control (ctrl) for 24 hours. Nuclear (N) and cytoplasmic (C) fractions of protein lysates were immunoblotted with the indicated antibodies. Nemo and Parp serve as cytoplasmic and nuclear loading controls respectively. (B) QPCR analysis of a subset of NF- κ B target genes in 5nM Bortezomib (BZ) treated KP cells at the indicated time points. Vehicle control is set to 1. (C) Bortezomib induces apoptosis in KP and KPM (*Kras*^{LSL-G12D/wt}; *p53*^{R127H/-}) cells. Cells were treated with 5nM Bortezomib for 24 hours and protein lysates were immunoblotted with cleaved caspase 3 (CC3) and Tubulin antibodies. (D) Quantification of cell death in Bortezomib treated cells. Cells were treated with the indicated concentrations of Bortezomib for 24 hours and dead cells were quantified by Trypan blue staining. Error bars are s.d. (n=3).

Fig. 2

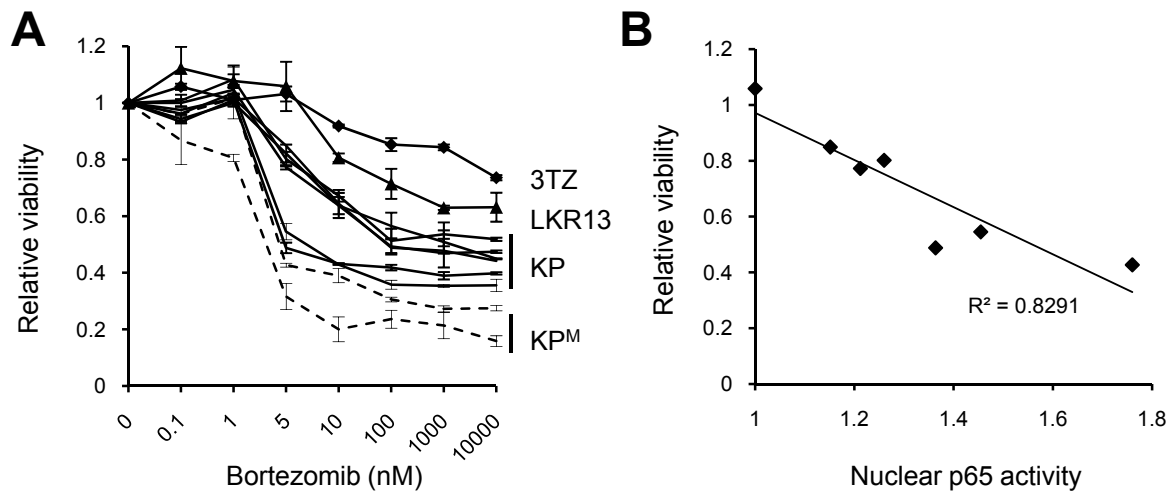


Figure 2. Bortezomib sensitivity correlates with basal NF- κ B activity in KP lung adenocarcinoma cell lines. (A) Relative cell viability in cell lines treated with increasing doses of Bortezomib for 24 hours. 3TZ, diamond; LKR13, triangle; KP, solid lines; KPM, dashed lines. Error bars are s.d. (n=3). **(B)** Lung cancer cell lines with high basal NF- κ B activity were sensitive to Bortezomib. NF- κ B p65 DNA binding activity was determined by ELISA from nuclear extracts of KP cell lines and LKR13 cells (set as 1). Relative viability was measured after 5nM Bortezomib treatment as in (A).

Fig. 3

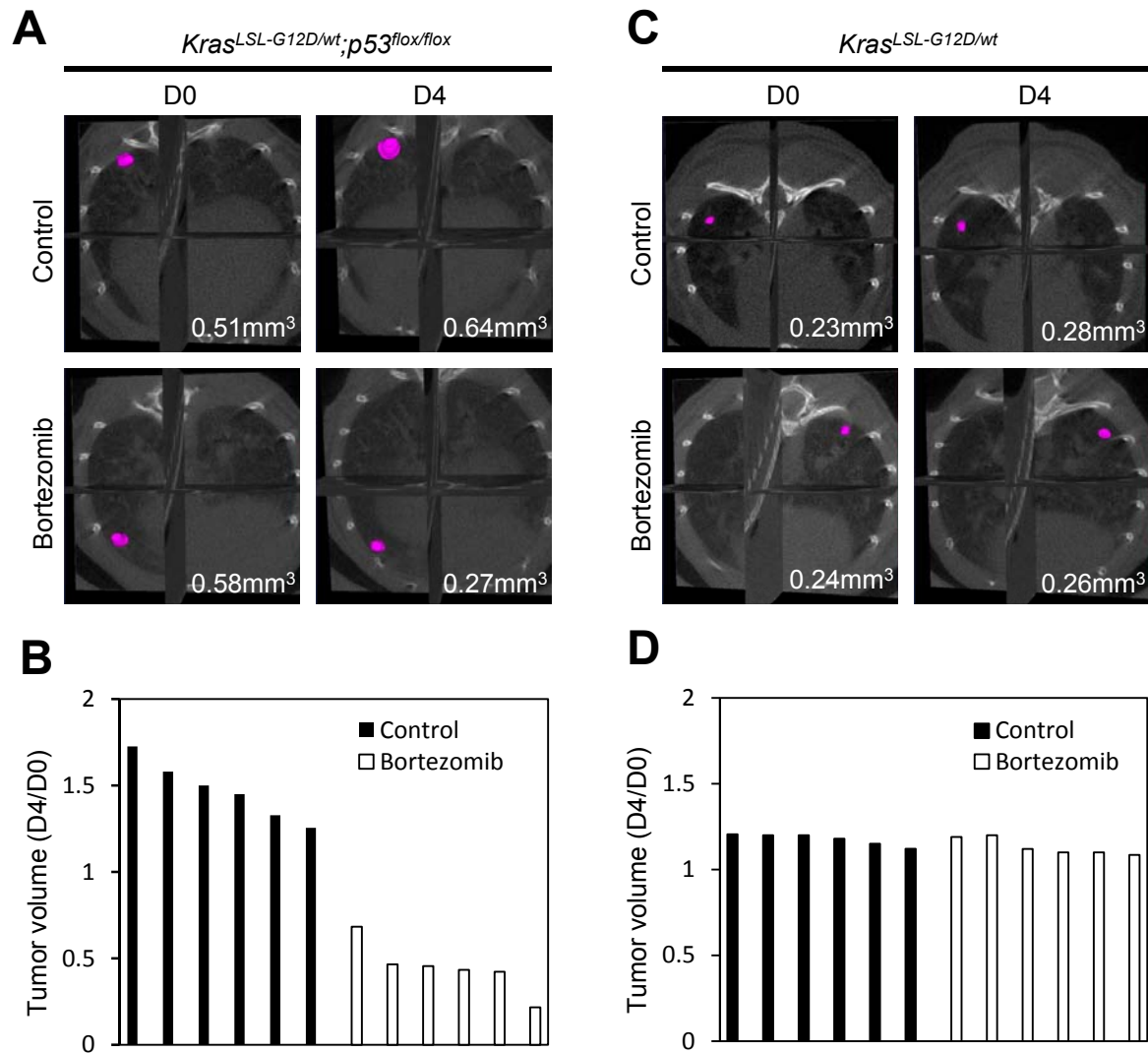


Figure 3. Bortezomib induces acute lung tumor regression in *Kras^{LSL-G12D/wt};p53^{flox/flox}* (KP) but not in *Kras^{LSL-G12D/wt}* (K) mice. (A,C) Representative microCT images (n=6) of KP (A) and K (C) lung tumors prior to treatment (D0) and 4 days (D4) after a single dose of vehicle control or Bortezomib. (B,D), Quantification of tumor volume change (D4 compared to D0) in control and Bortezomib treated mice. Each bar represents an individual tumor. $p < 10^{-6}$ in KP mice (B), $p > 0.05$ in K mice (D).

Fig. 4

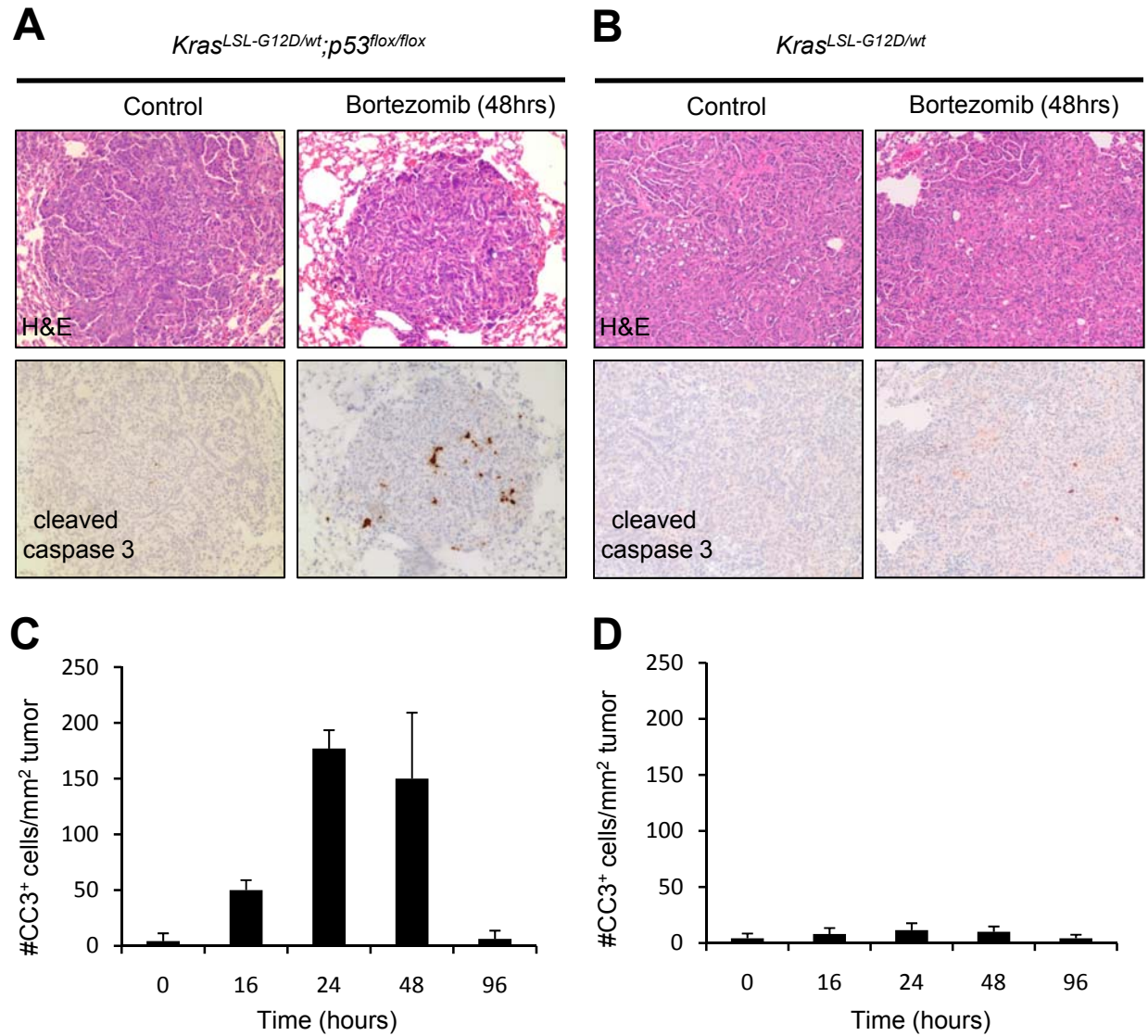


Figure 4. Bortezomib induces apoptosis in KP lung tumors. (A-B), H&E and cleaved caspase 3 (CC3) immunohistochemistry staining (200x) in vehicle control and Bortezomib treated KP (A) and K (B) lung tumors. **(C-D)** Quantification of CC3 positive cells in Bortezomib treated KP (C) and K (D) lung tumors at indicated time points. “0 hour” represents vehicle control treated tumors. Error bars are s.d. (n>10 for each time point).

Fig. 5

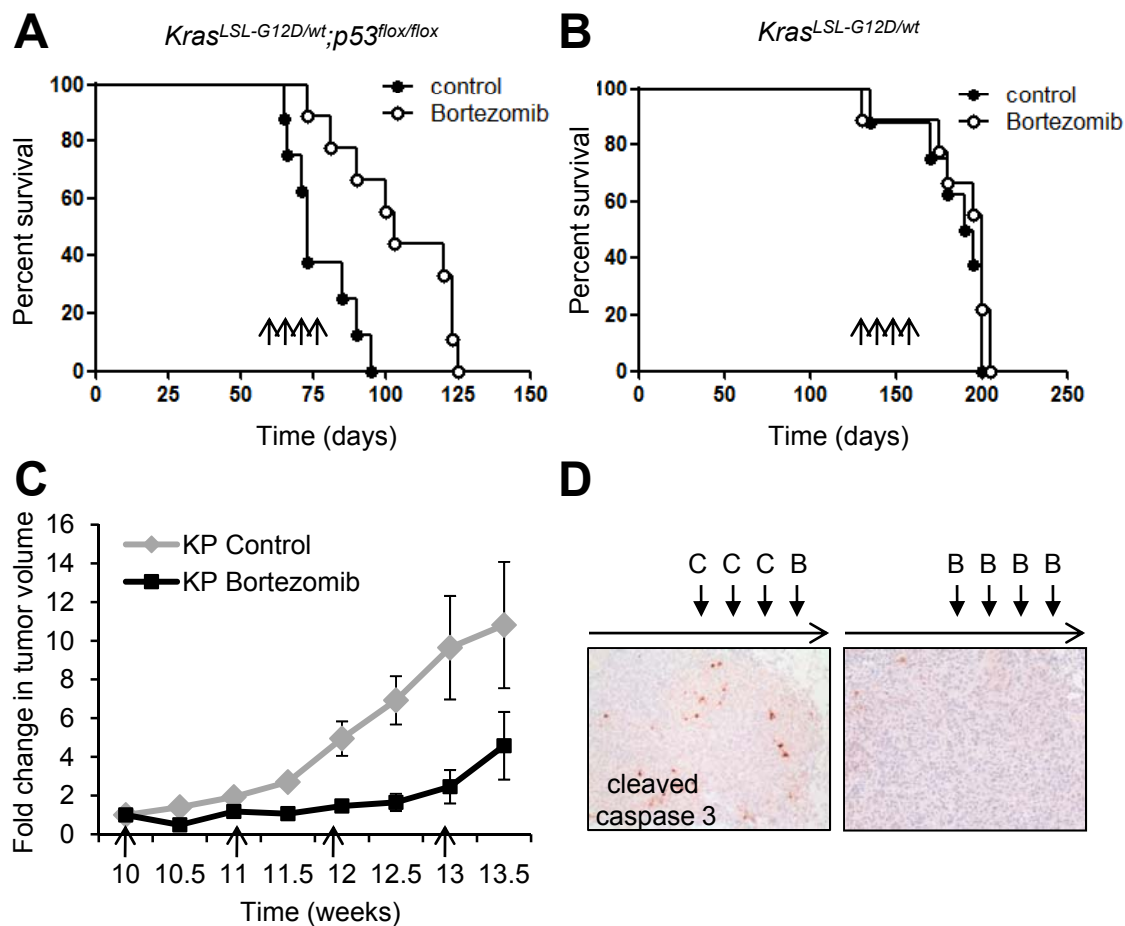


Figure 5. Bortezomib increases survival in KP mice. (A-B), Kaplan-Meier survival curve of vehicle control and Bortezomib treated KP (A) and K (B) mice. Arrows indicate weekly 1mg/kg Bortezomib regimen. **(C)** Quantification of lung tumor volume of control and Bortezomib treated KP mice. From 10 weeks post Adeno-Cre infection, lungs were imaged by microCT to measure individual tumour volumes (n=4). Data points represent means of fold change and s.d. relative to 10 weeks (set to 1). Arrows indicate Bortezomib injection. **(D)** Cleaved caspase 3 (CC3) staining (200x) in lung tumors receiving 3 doses of control ("C") and 1 final dose of Bortezomib ("B") (left) or 4 doses of Bortezomib (right). Tumors were harvested 48 hours after the last treatment (n=4).

Fig. 6

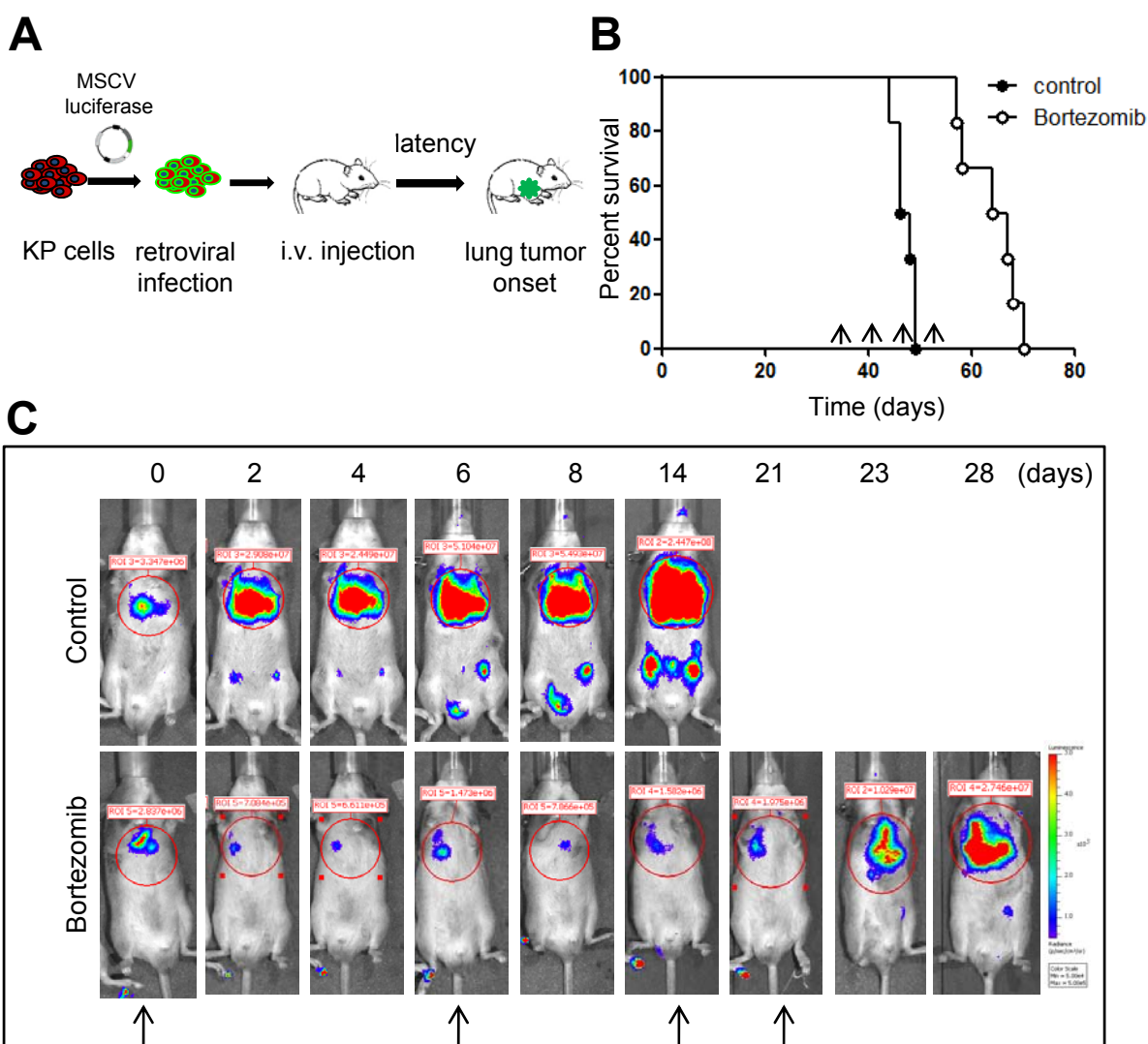


Figure 6. Imaging Bortezomib response and resistance in an orthotopic lung tumor model. (A) Experimental design. Lung cancer cells derived from KP tumors were infected with a retrovirus expressing luciferase and transplanted into immunocompetent recipient mice by tail vein injection. **(B)** Kaplan-Meier survival curve of control and Bortezomib treated recipient mice ($n=6$, $p=1.4 \times 10^{-5}$). 10,000 cells were transplanted and treatment started after 35 days. **(C)** Representative bioluminescence imaging of recipient mice ($n=6$) treated with vehicle control or Bortezomib as in (B). D0 refers to the first treatment. Arrows indicate weekly Bortezomib regimen.

Fig. 7

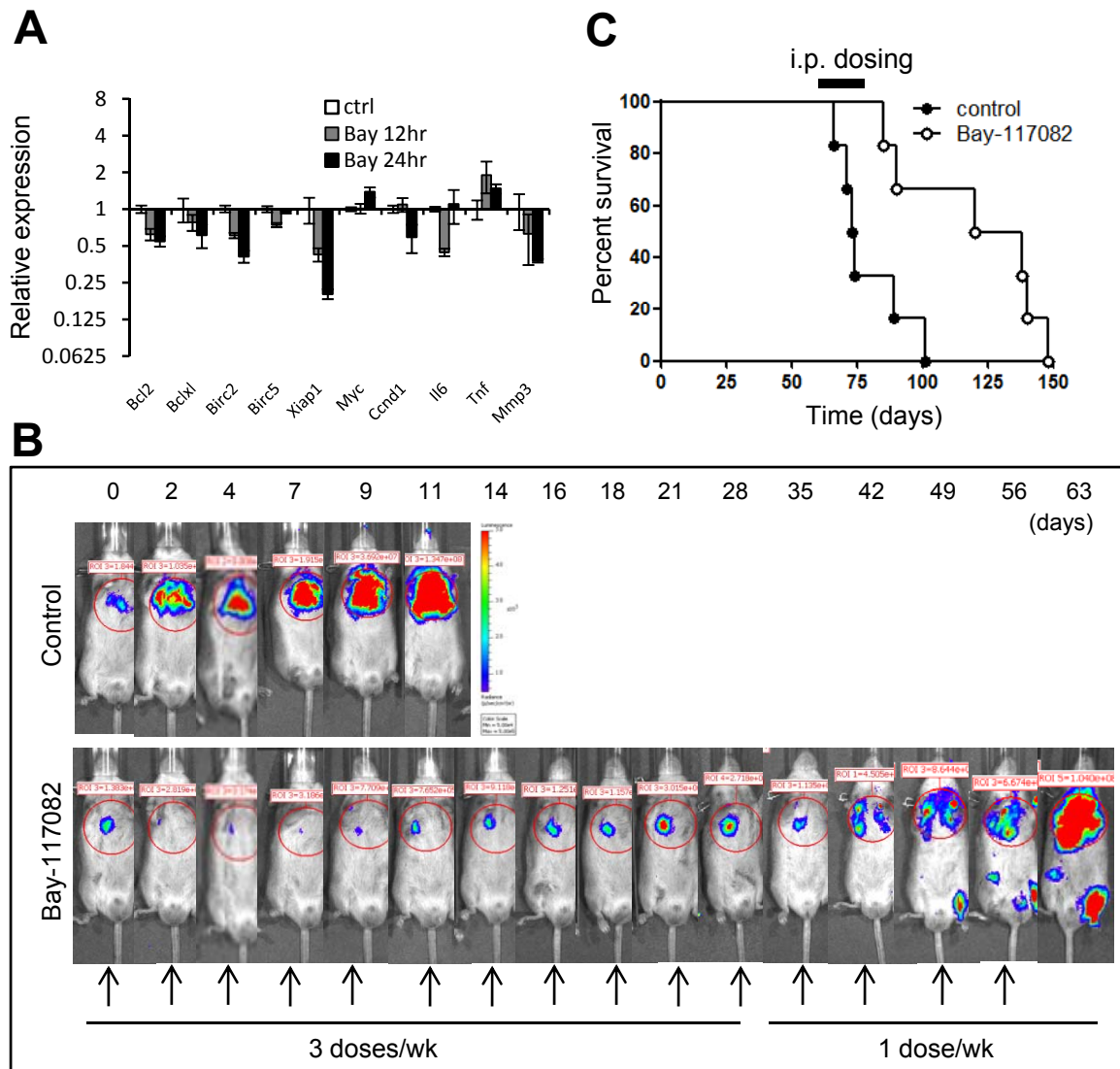
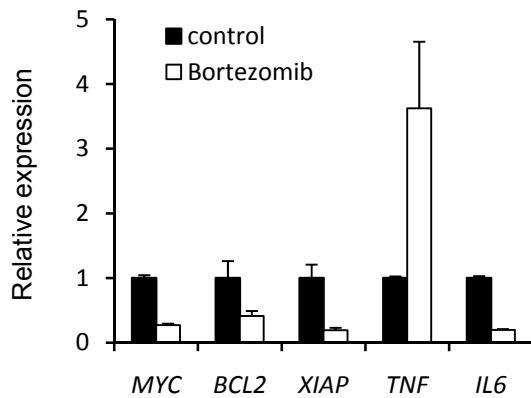


Figure 7. The NF- κ B inhibitor Bay-117082 leads to lung tumor regression *in vivo*. (A) QPCR analysis in KP cells treated with 10 μ M Bay-117082 for indicated hours (hr). Error bars are s.d. (n=3). (B) Bay-117082 treatment leads to lung tumors regression and delays tumor progression in the orthotopic lung tumor model. 50,000 luciferase tagged KP cells were transplanted into recipient mice (n=6) and treatment started at 19 days post transplantation (set at D0). Mice were treated with vehicle control or 10mg/kg Bay-117082 by i.p. injection, and imaged at the indicated time points. Arrows indicate Bay-117082 injections. (C) Bay-117082 prolongs survival in the KP model (n=6, p=0.008). "i.p. dosing" indicates 3 doses per week treatment.

Fig. S1

A.



B.

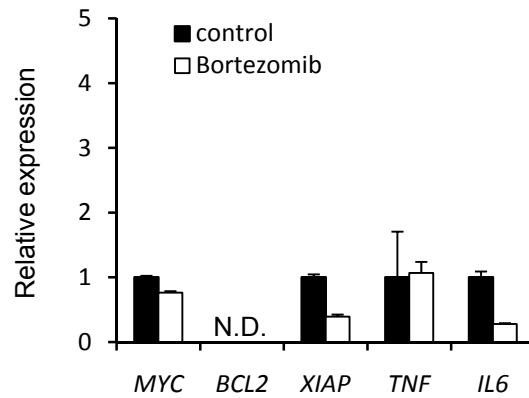


Figure S1. Bortezomib inhibits NF-κB signaling in human NSCLC cells. H2122 (*KRAS*^{G12C};*TP53*^{C176F/Q16L}) (**A**) and H2009 (*KRAS*^{G12A};*TP53*^{R273L}) (**B**) cell lines were treated with vehicle control or 10nM Bortezomib for 24 hours. NF-κB target gene expression was measured by QPCR. Error bars are s.d. (n=3). N.D. denotes not detectable. Mutation information is from the Sanger COSMIC database.

Fig. S2

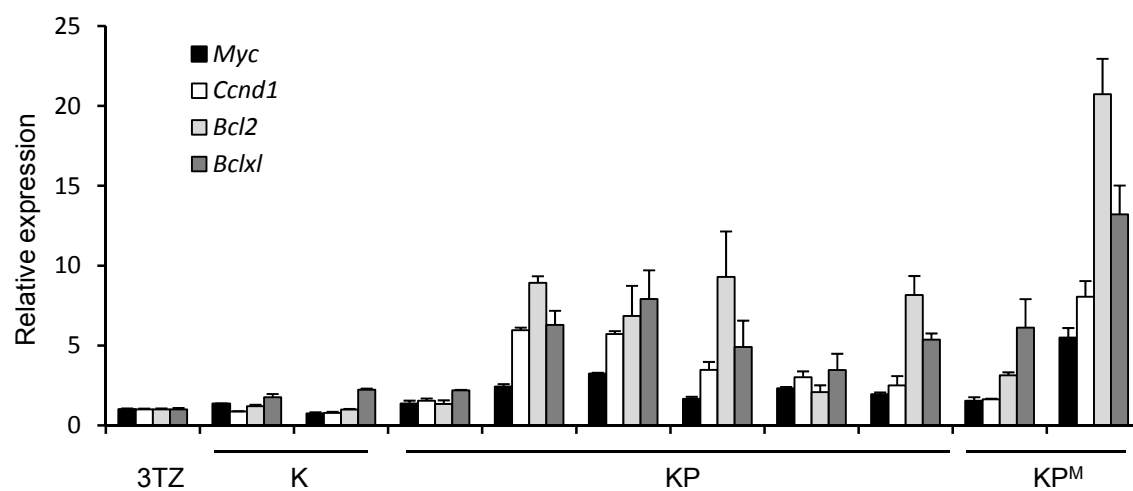
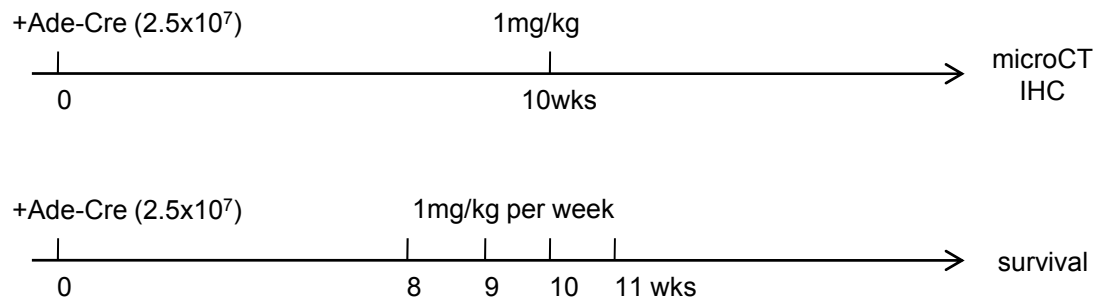


Figure S2. QPCR analysis of NF- κ B target genes expression in murine lung adenocarcinoma cell lines. Values in the 3TZ fibroblast cell line is set to 1. Error bars are s.d. (n=3).

Fig. S3

A. *Kras*^{LSL-G12D/wt}; *p53*^{flx/flx}



B. *Kras*^{LSL-G12D/wt}

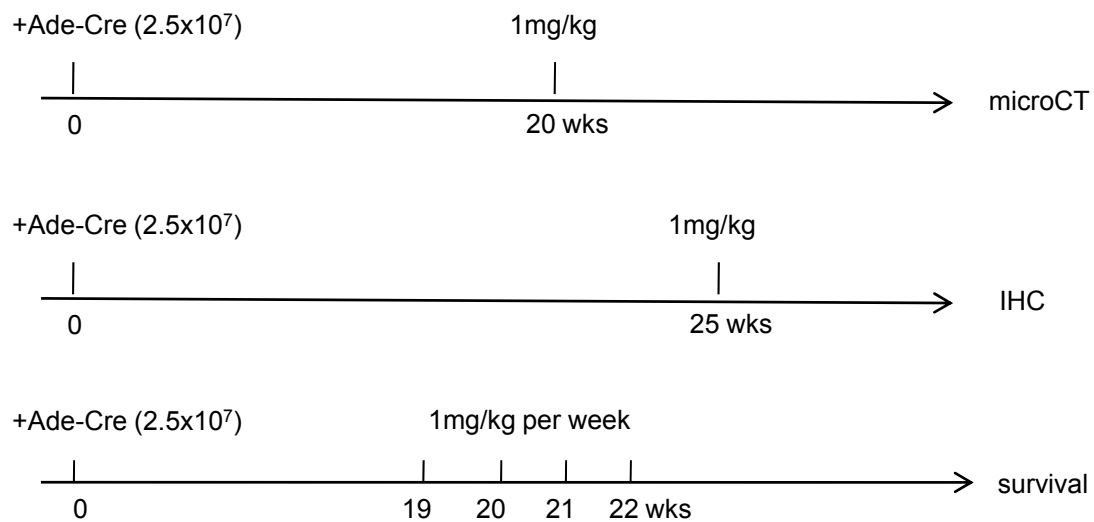


Figure S3. Bortezomib regimen in (A) KP and (B) K mice.

Fig. S4

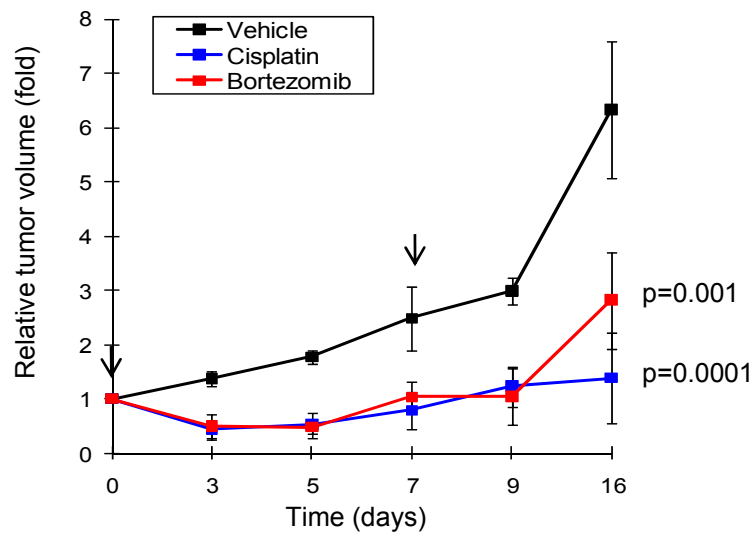


Figure S4. Bortezomib reduces tumor volume in a subcutaneous tumor model. 1×10^6 KP lung cancer cells were injected subcutaneously into NCR nu/nu mice. Tumor volume was quantified by caliper measurements. Treatments started when tumors reached $\sim 100 \text{ mm}^3$ (set to 1 in tumor volume axis and 0 days in time axis). Arrows indicate Bortezomib (1mg/kg) or Cisplatin (7mg/kg) injections. Error bars are s.d (n=4).

Fig. S5

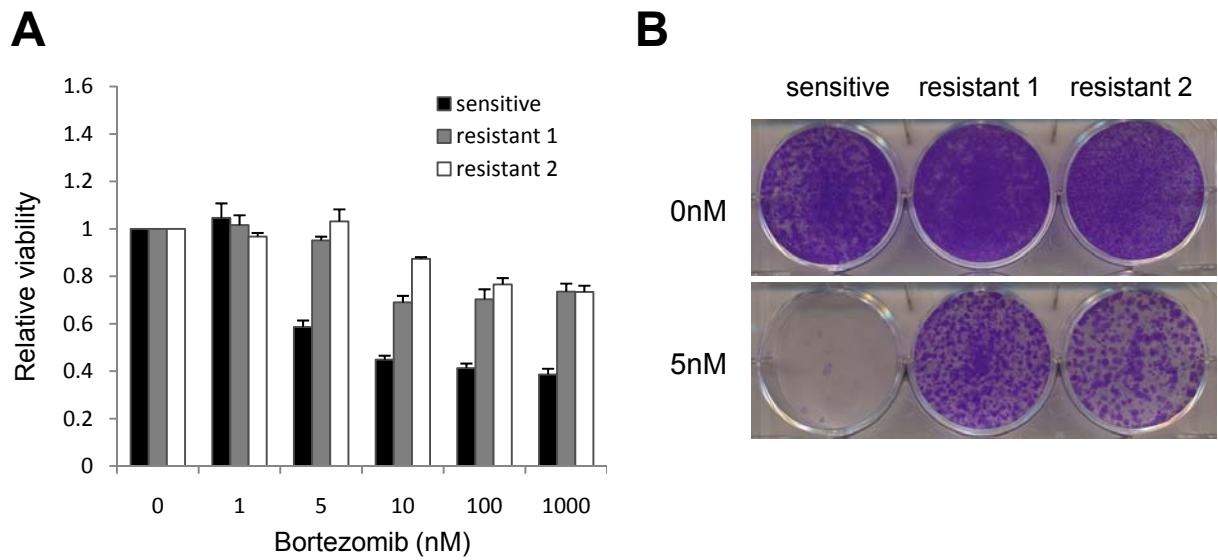


Figure S5. Generating Bortezomib-resistant KP cell lines. (A) Relative cell viability in cell lines treated with increasing doses of Bortezomib for 24 hours. Cells lines were outgrown from Bortezomib-resistant orthotopic tumors (resistant 1&2) or sensitive tumors (sensitive) as in Fig. 6C. Error bars are s.d. (n=3). **(B)** Colony formation assay in Bortezomib-resistant cells. 10^4 cells were plated in 6-well plate and treated with indicated drug concentration. Plates were stained 7 days later with crystal violet solution. Drug-containing medium was refreshed every 4 days.

Fig. S6

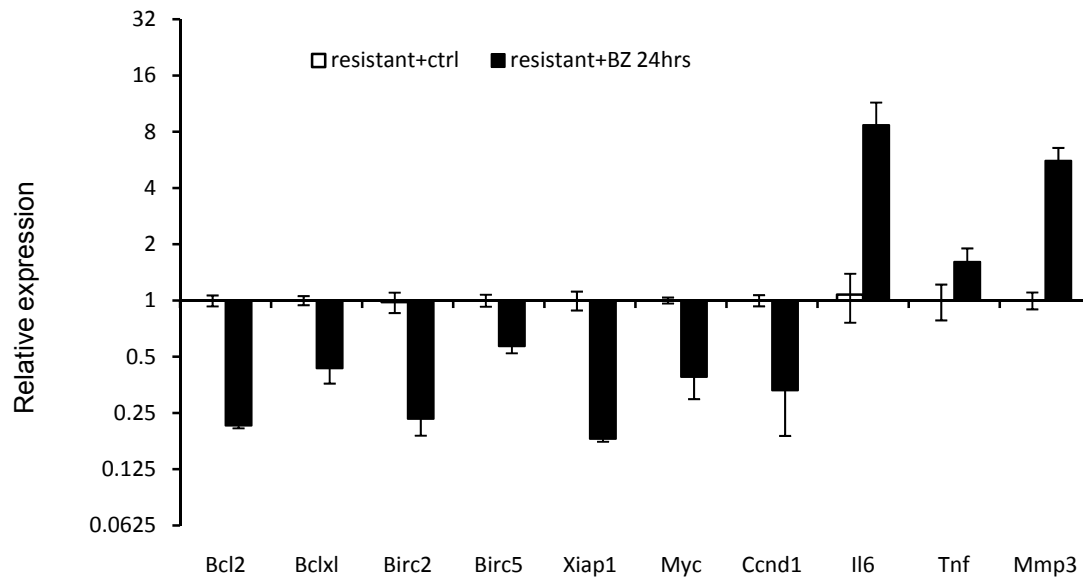


Figure S6. Bortezomib-resistant KP cell lines showed down-regulation of NF-κB targets regulating apoptosis and cell cycle upon drug treatment. A representative resistant cell line was treated with control or 5nM Bortezomib for 24 hours. Gene expression level was measured by QPCR and normalized to control-treated cells (set to 1). Error bars are s.d. (n=3).

Fig. S7

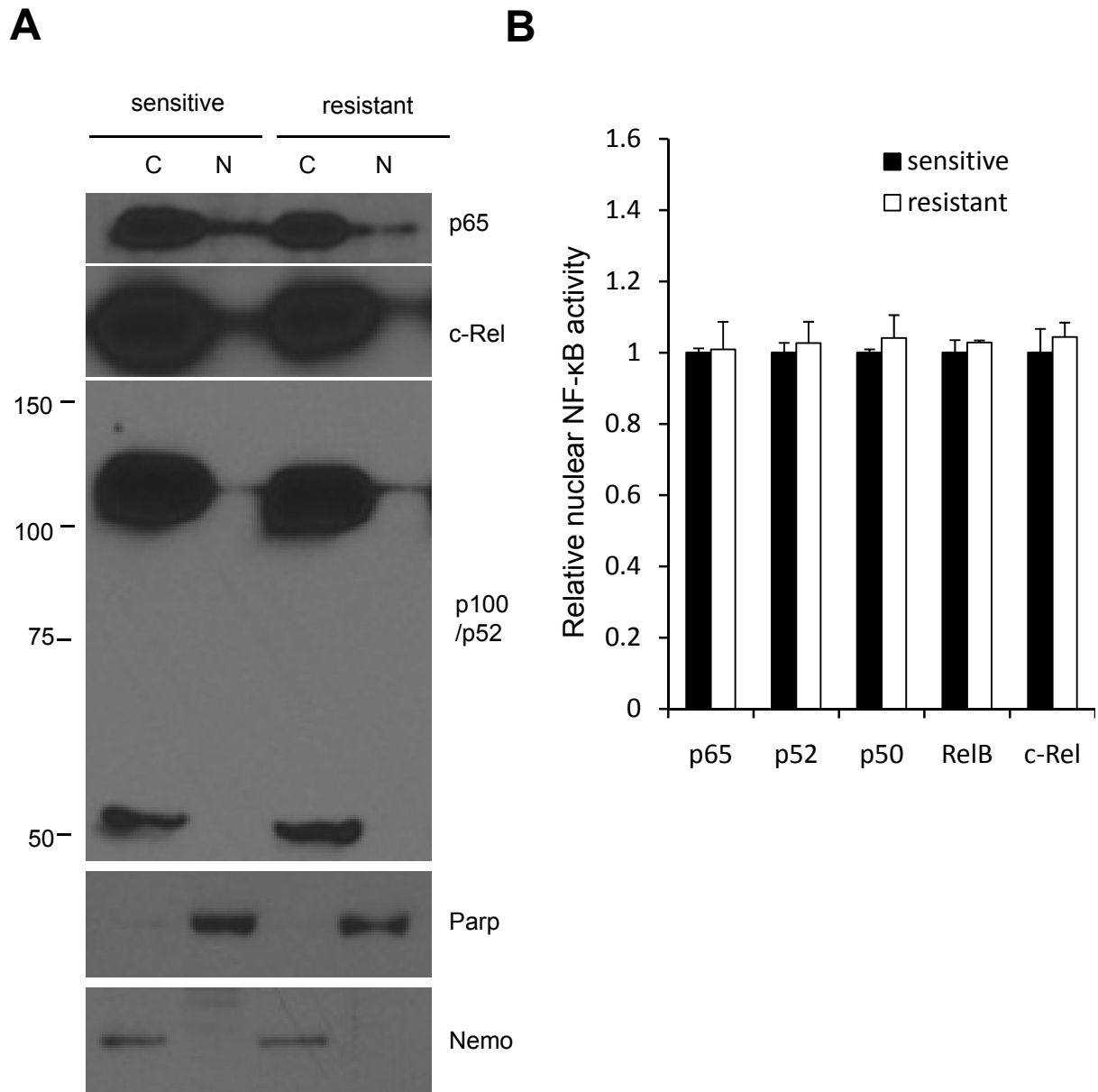


Figure S7. Nuclear NF- κ B levels in Bortezomib-resistant and sensitive KP cell lines. (A) Nuclear (N) and cytoplasmic (C) fractions of protein lysates were immunoblotted with the indicated antibodies. Nemo and Parp serve as cytoplasmic and nuclear loading controls respectively. **(B)** Activity of NF- κ B in the nuclear extract was measured by ELISA assay. Values in the sensitive cell line is set to 1. Error bars are s.d. ($n=3$, $p>0.05$ for all NF- κ B subunits).

Fig. S8

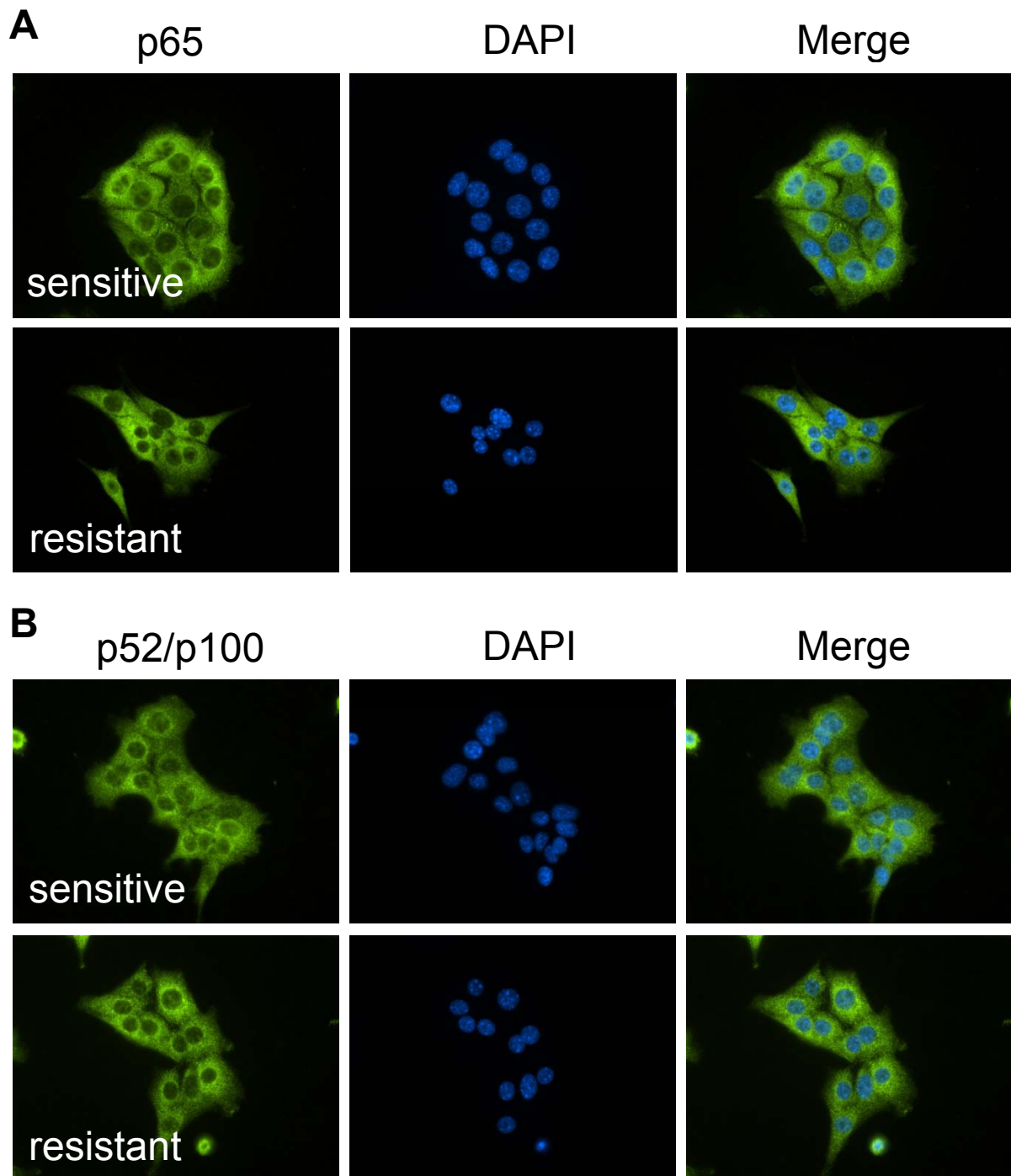


Figure S8. Immunofluorescence in Bortezomib-resistant and sensitive KP cell lines. Fixed cells were stained with antibodies for p65 (**A**) and p52/p100 (**B**) (an antibody recognizing both the p52 and its precursor p100) and Alexa-488 secondary antibody (green). Nucleus were stained with DAPI (blue). Images are 400x magnitude.

Fig. S9

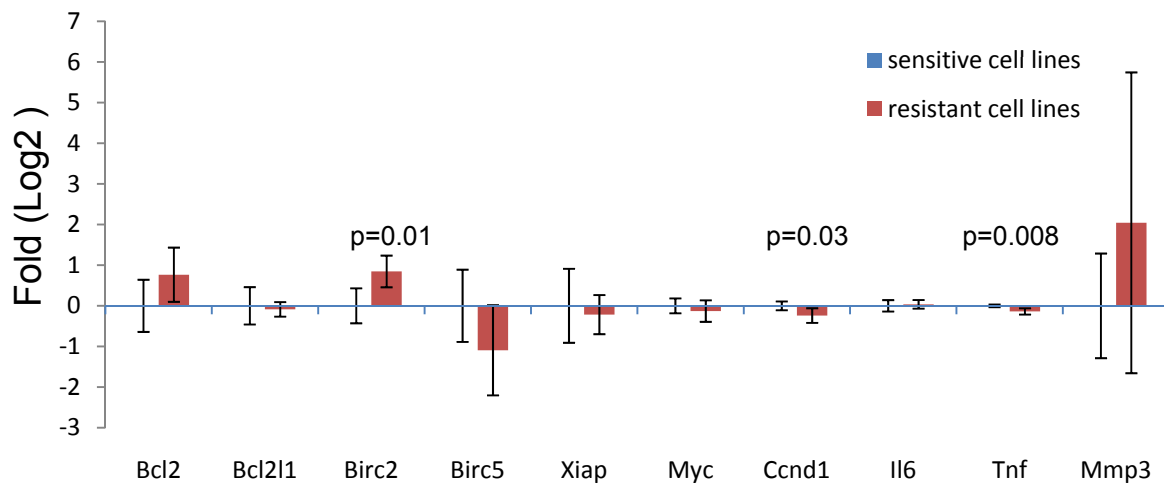


Figure S9. Transcriptional profile of NK-κB targets in Bortezomib-resistant KP cell lines. Gene expression level was quantified by QPCR in four sensitive and four resistant KP cell lines. The average of sensitive cells is set to 1. p values indicate genes significantly different in resistant cells. Error bars are s.d. (n=4).

Fig. S10

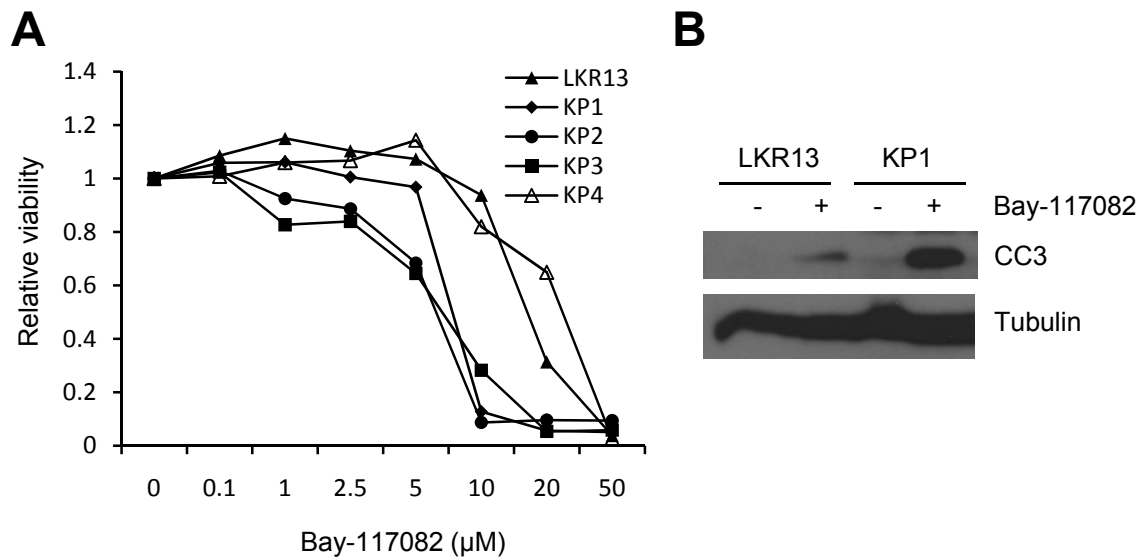
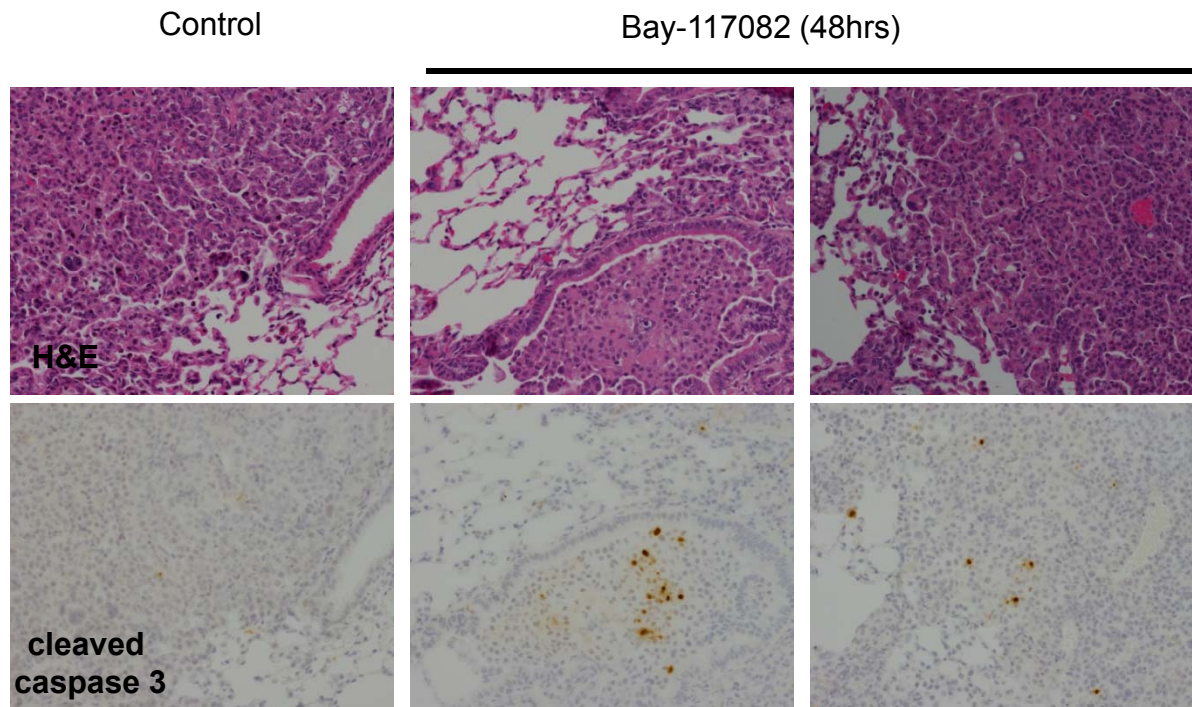


Figure S10. Bay-117082 induces cell death in KP cells. (A) Relative cell viability in cell lines treated with increasing doses of Bay-117082 for 48 hours. **(B)** Bay-117082 induces apoptosis in KP cells. Cells were treated with 10 μM Bay-117082 for 48 hours. Protein lysates were immunoblotted with cleaved caspase 3 (CC3) and Tubulin antibodies.

Fig. S11

A



B

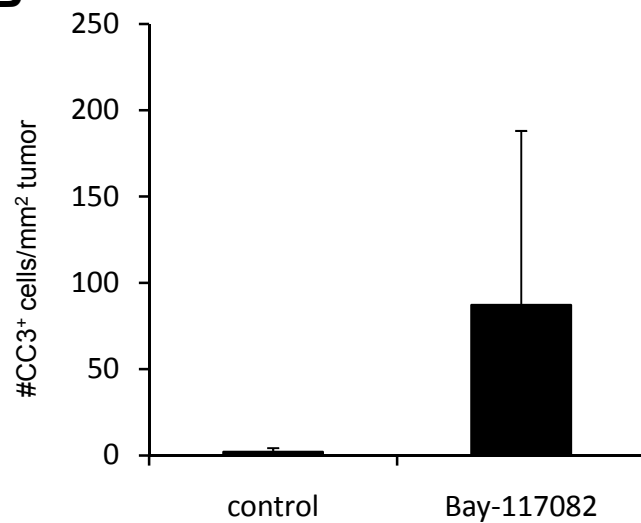


Figure S11. Bay-117082 induces apoptosis in KP lung tumors. (A), H&E and cleaved caspase 3 (CC3) immunohistochemistry staining (200x) in vehicle control and Bay-117082 treated KP lung tumors (10mg/kg, 48hrs). **(B)** Quantification of CC3 positive cells. Error bars are s.d. ($p < 0.05$).